AD-A073 318   NAVAL SURFACE WEAPONS CENTER WHITE OAK LAB SILVER SP--ETC F/G 20/8
RIGID-ROTOR EQUILIBRIUM OF INTENSE RELATIVISTIC ELECTRON BEAM.(U)
MAR 79 H S UHM
UNCLASSIFIED   NSWC/WOL/TR-78-182   NL

1 OF 1
AD
A073318

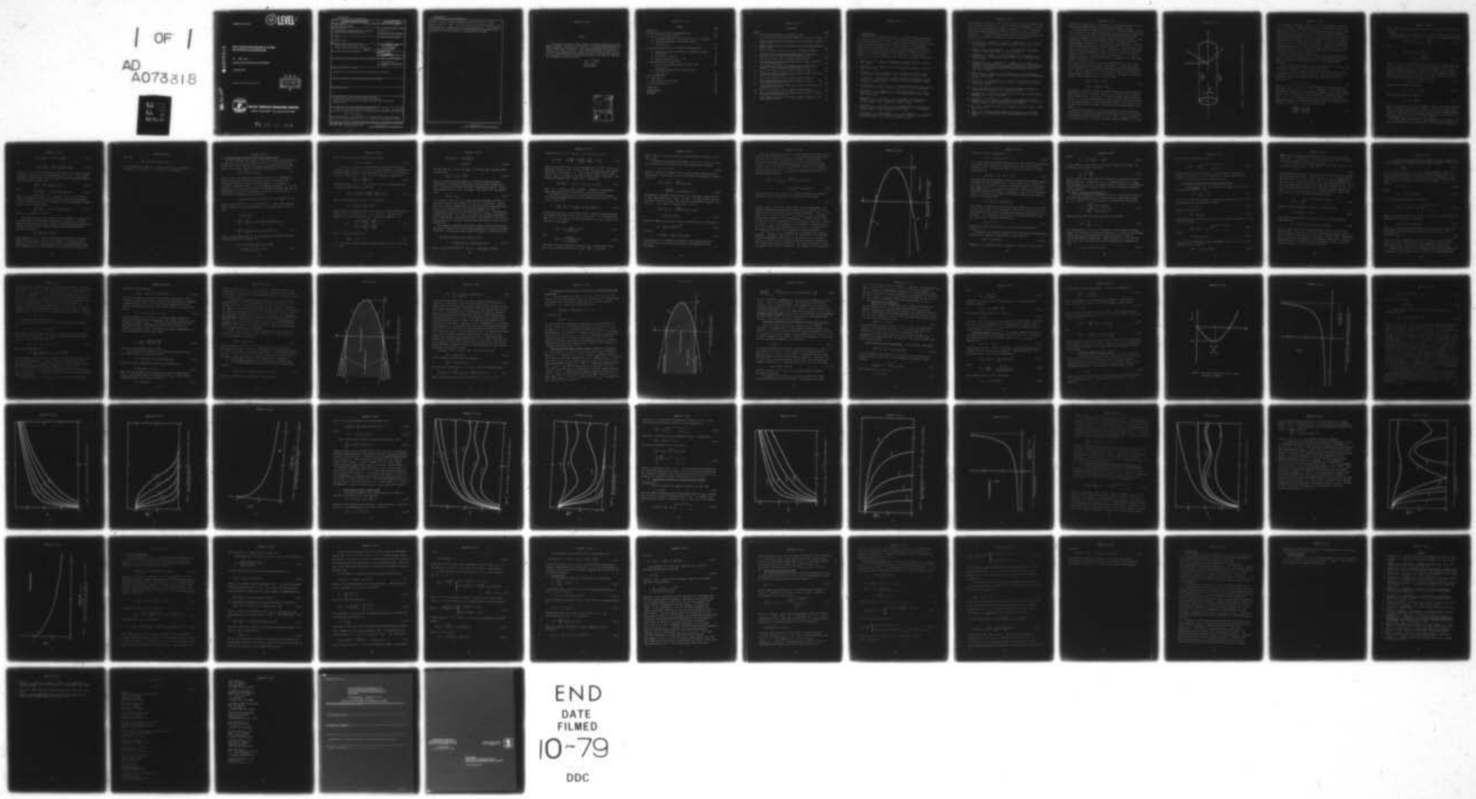

END
DATE
FILMED
10-79
DDC

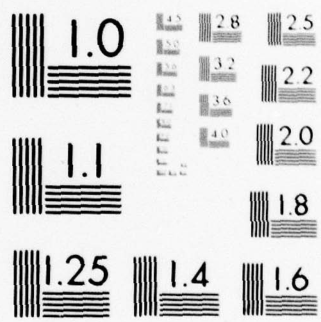

MICROCOPY RESOLUTION TEST CHART
NATIONAL BUREAU OF STANDARDS-1963-A

NSWC/WOL TR 78-182

RIGID-ROTOR EQUILIBRIUM OF INTENSE RELATIVISTIC ELECTRON BEAM

BY HAN S. UHM

RESEARCH AND TECHNOLOGY DEPARTMENT

15 MARCH 1979

Approved for public release, distribution unlimited.

NAVAL SURFACE WEAPONS CENTER

Dahlgren, Virginia 22448 • Silver Spring, Maryland 20910

UNCLASSIFIED

SECURITY CLASSIFICATION OF THIS PAGE (When Data Entered)

REPORT DOCUMENTATION PAGE		READ INSTRUCTIONS BEFORE COMPLETING FORM
1. REPORT NUMBER (14) NSWC/WOL/TR-78-182	2. GOVT ACCESSION NO.	3. RECIPIENT'S CATALOG NUMBER
4. TITLE (and Subtitle) (6) RIGID-ROTOR EQUILIBRIUM OF INTENSE RELATIVISTIC ELECTRON BEAM		5. TYPE OF REPORT & PERIOD COVERED (9) Final rept.
		6. PERFORMING ORG. REPORT NUMBER
7. AUTHOR(s) (10) Han S. Uhm		8. CONTRACT OR GRANT NUMBER(s)
9. PERFORMING ORGANIZATION NAME AND ADDRESS Naval Surface Weapons Center White Oak, Silver Spring, Maryland 20910		10. PROGRAM ELEMENT, PROJECT, TASK AREA & WORK UNIT NUMBERS (16) 61152N; ZR00001 (17) ZR01109; R0123
11. CONTROLLING OFFICE NAME AND ADDRESS		12. REPORT DATE (11) 15 March 1979
		13. NUMBER OF PAGES 71 (12) 72p.
14. MONITORING AGENCY NAME & ADDRESS (if different from Controlling Office)		15. SECURITY CLASS. (of this report) UNCLASSIFIED
		15a. DECLASSIFICATION/DOWNGRADING SCHEDULE

16. DISTRIBUTION STATEMENT (of this Report)

Approved for Public Release; distribution unlimited

17. DISTRIBUTION STATEMENT (of the abstract entered in Block 20, if different from Report)

18. SUPPLEMENTARY NOTES

19. KEY WORDS (Continue on reverse side if necessary and identify by block number)

Electron Beam, Relativistic Electron Motion, Rigid-Rotor Equilibrium, Thermal Equilibrium Properties, Intense Beam

20. ABSTRACT (Continue on reverse side if necessary and identify by block number)

The various equilibrium properties of an intense, continuous, relativistic electron beam with a distribution function of the form

$$f_b^0 = F(H-\omega_b P_\theta, P_z)$$

are investigated. This choice of f_b° allows for a mean azimuthal rotation of the beam electrons, ω_b. Beam equilibrium properties, including an axial velocity profile, $V_{zb}^\circ(r)$, an azimuthal velocity

DD FORM 1 JAN 73 1473 EDITION OF 1 NOV 65 IS OBSOLETE S/N 0102-014-6601

UNCLASSIFIED

SECURITY CLASSIFICATION OF THIS PAGE (When Data Entered)

391 596

profile, $V^{o}_{\theta b}(r)$, a beam temperature profile, $T^{o}_{b}(r)$, a beam density profile, $n^{o}_{b}(r)$, and equilibrium self-field profiles, are calculated for a broad range of system parameters. The necessary and sufficient conditions for radially-confined equilibria are obtained for various electron distribution functions.

SUMMARY

Understanding of the equilibrium properties of intense relativistic electron beams is extremely important in various areas, including microwave generation and beam propagation in the atmosphere. This report examines the equilibrium properties of the intense relativistic electron beam described by the rigid-rotor equilibrium distribution function. Beam properties including an axial velocity profile, a beam temperature, a beam density, and equilibrium self-field profiles are calculated for a broad range of system parameters. This work was supported by Independent Research at the center.

Paul R. Wessel

PAUL R. WESSEL
By direction

CONTENTS

ILLUSTRATIONS

1. INTRODUCTION

This work is a theoretical study of the equilibrium properties[1-5] of a relativistic electron beam. The major recent interest in the equilibrium properties of relativistic electron beams originates from several diverse research areas. These include: (a) fundamental experimental and theoretical studies of equilibrium and stability properties of magnetically confined nonneutral plasmas in mirror,[6-8] cusped,[9] and uniform[5] magnetic field geometries, (b) research on collective - effect accelerators that utilize the intense self fields

---

1. Davidson, R. C., Theory of Nonneutral Plasma (Benjamin, Reading, MA., 1974).

2. Bennett, W. H., "Magnetically Self-Focussing Streams," Phys. Rev. 45, 1934, p 890.

3. Hammer, D. A., and Rostoker, N., "Propagation of High Current Relativistic Electron Beams," Phys. Fluids 13, 1970, p. 1831.

4. Gratreau, P., "Generalized Bennett Equilibria and Particle Orbit Analysis of Plasma Columns Carrying Ultra-High Currents," Phys. Fluids 21, 1978, p 1302.

5. Davidson, R. C., and Uhm, H. S., "Thermal Equilibrium Properties of an Intense Relativistic Electron Beam," phys. Fluids, in press 1979.

6. Armstrong, C. M., Hammer, D. A., and Trivelpiece, A. W., "Non-neutral Electron Plasma With a 2.5 MeV Mean Energy," Phys. Lett. A55, 1976, p 413.

7. Davidson, R. C., and Uhm, H. S., "Influence of Strong Self-Electric Fields on Ion Resonance Instability in a Nonneutral Plasma Column," Phys. Fluids, 20, 1977, p 1938.

8. Davidson, R. C., and Uhm, H. S., "Influence of Finite Ion Larmor Radius Effects on the Ion Resonance Instability in a Nonneutral Plasma Column," Phys. Fluids, 21, 1978, p 60.

9. Striffler, C. D., Kapetnnakos, C. A., and Davidson, R. C., "Equilibrium Properties of a Rotating Nonneutral E Layer in a Cusped Magnetic Field," Phys. Fluids, 18, 1975, p 1374.

of an electron cluster,[10] the electron cyclotron resonance mode (the Auto Resonant Accelerator),[11] and the converging waveguide,[12] (c) research on the high-power microwave generation[13-15] and (d) studies of electron beam propagation through a neutral gas or background plasma.[16-20] Although these research areas have different goals and objectives, they have in common the need to understand the

---

10. Destler, W. W., Uhm, H. S., Kim, H., and Reiser, M. P., "Study of Collective Ion Acceleration in Vacuum" J. Appl. Phys. in press (1979).

11. Sloan, M. W., and Drummond, W. E., "Autoresonant Accelerator Concept," Phys. Rev. Lett. 31, 1973, p 1234.

12. Sprangle, P., Drobot, A., and Manheimer, W., "Collective Ion Acceleration in a Converging Wave Guide," Phys. Rev.Lett. 36, 1976, p 1180.

13. Granatstein, V. L., Sprangle, P., Parker, R. K., Pasour, J., Herndon, M., Schlesinger, S. P., and Sefter, J. L., "Realization of Relativistic Mirror; Electromagnetic Backscattering from the Front of a Magnetized Relativistic Electron Beam," Phys. Rev. A14, 1976, p 1194.

14. Flyagin, V. A., Gaponov, A. V., Petelin, M. I., and Yulpatov, V. K., "The Gyroton," IEEE Trans. Microwave Theory and Techniques, MTT-25, 1977, p 514.

15. Uhm, H. S., and Davidson, R. C., "Quasi-Linear Theory of Cyclotron Maser Instability," Phys. Fluids 22, in press (1979) and references therein.

16. Reiser, M. "Laminar-Flow Equilibria and Limiting Currents in Magnetically Focused Relativistic Beams", Phys. Fluids 20, 477 (1977).

17. Kligman, R. L., "Electric Conductivity in a Beam, Plasma System," NSWC/WOL TR 77-146, 15 Sep 1977.

18. Briggs, R. J., Hester, R. E., Lauer, E. J., Lee, E. P., and Spoerlein, R. L., "Radial Expansion of Self-Focused, Relativistic Electron Beams," Phys. Fluids, 19, 1976, p 1007.

19. Lee, E. P., "Kinetic Theory of a Relativistic Beam," Phys. Fluids 19, 1976, p 60.

20. Lampe, M., "Energy Moment Method for Straggling of an Ultra-Relativistic Electron Beam," NRL Memorandum Report 3221, Feb 1976.

equilibrium properties of a relativistic electron beam that is characterized by intense self electric and self magnetic fields.

The theoretical analysis of relativistic electron beams is carried out, neglecting the atomic process and discrete particle interactions (i.e., binary collisions), because the collective processes are assumed to dominate on the time and length scales of interest. The equilibrium properties are examined within the framework of the Vlasov-Maxwell equations.[1] The analysis is carried out for an infinitely long electron beam as shown in Figure 1. The mean radius of the electron beam is denoted by a. The mean motion of the electron beam is in the azimuthal and axial directions, producing the self magnetic fields. Cylindrical polar coordinates (r, θ, z) are introduced with the z axis along the axis of symmetry; r is the radial distance from the z axis,
and θ is the polar angle in the plane perpendicular to the z axis. The relativistic electron beam is immersed in a cylindrical background plasma and is partially charge neutralized by extra positive ions. We also expect that the background plasma has an additional equal number of positive ions and electrons. The positive ions are assumed to be immobile $(m_i \to \infty)$. Thus we have

$$\begin{aligned} n_e^0(r) &= n_b^0(r) + n_p^0(r), \\ n_i^0(r) &= f_e n_b^0(r) + n_p^0(r), \end{aligned} \tag{1.1}$$

where $n_b^0(r)$ and $n_p^0(r)$ are the equilibrium beam and plasma densities, respectively, $n_e^0(r)$ and $n_i^0(r)$ are the total electron and ion densities, respectively, and f_e=const is the fractional charge neutralization. It is also assumed that the space current density generated by the beam electrons is partially neutralized by the return current of plasma electrons, with the fractional current neutralization f_m= const.

Equilibrium properties of the electron beam are calculated for the class of rigid-rotor equilibria described by kinetic equilibrium distributions of the form $f_b^0(H, P_\theta, P_z) = f_b^0(H - \omega_b P_\theta, P_z)$, where H is the total energy, P_θ is the canonical angular momentum, P_z is the

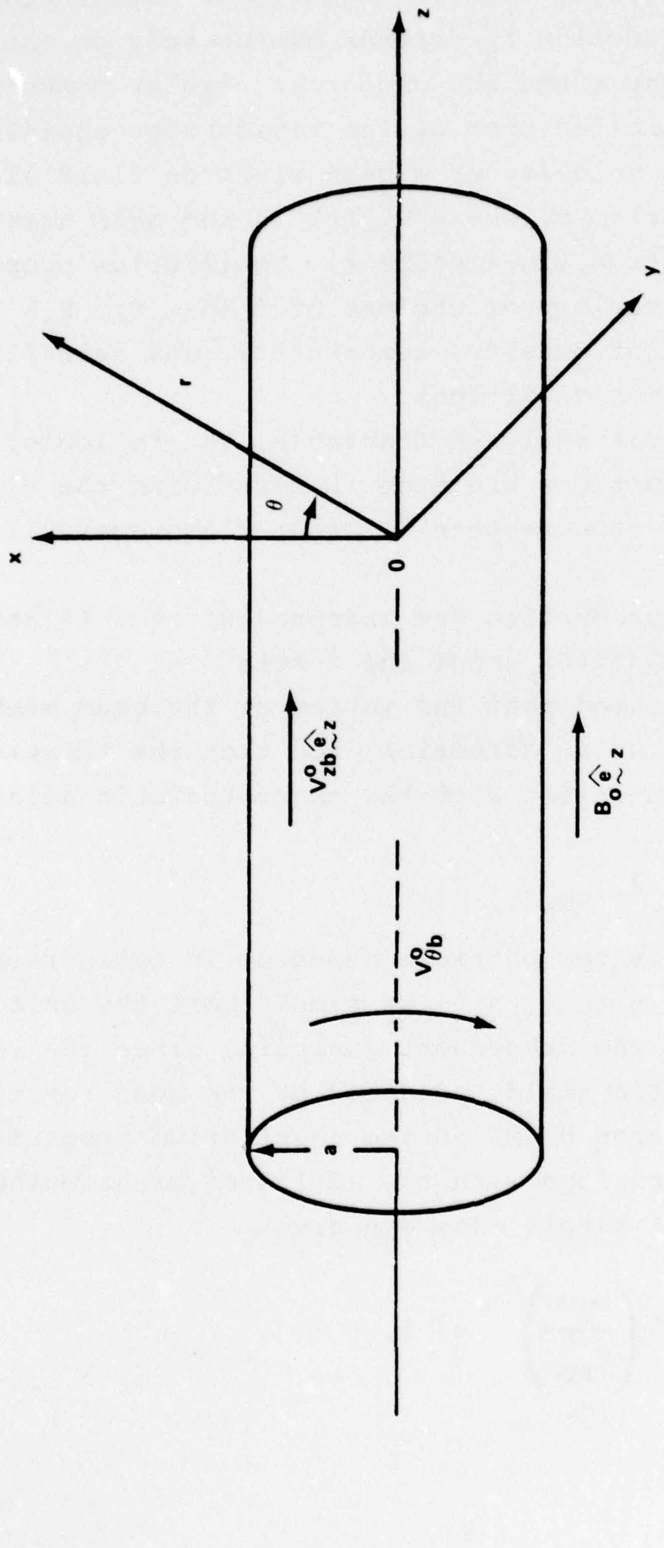

Figure 1. Equilibrium Configuration and Coordinate Systems

axial canonical momentum, and ω_b is the canonical angular velocity. It is worthwhile to emphasize that in rigid-rotor equilibrium, the electron distribution function f_b^0 depends exclusively on the linear combination of the energy H and the canonical angular momentum P_θ. One of the characteristic features of the rigid-rotor equilibrium is that the mean azimuthal velocity of a beam electron fluid element is rigid-rotor, i.e., $V_{\theta b}^0(r)=\omega_b r$, where $V_{\theta b}^0(r)$ is the mean azimuthal velocity of a beam electron fluid element. Equilibrium properties are investigated for a variety of choices of $f_b^0(H-\omega_b P_\theta, P_z)$ to determine the sensitivity of density, temperature, and self-field profiles to beam injection conditions.

To make the theoretical analysis tractable, the following additional simplifying assumptions are made in describing the electron beam equilibrium by the steady-state ($\partial/\partial t=0$) Vlasov-Maxwell equations;

(a) The equilibrium properties are independent of z ($\partial/\partial z=0$) and aximuthally symmetric ($\partial/\partial\theta=0$) about the z axis.

(b) It is further assumed that the motion of the beam electrons is predominately in the axial direction, and that the transverse momentum is small in comparison with the characteristic axial momentum, i.e.,

$$p_r^{\ 2} + p_\theta^{\ 2} \ll p_z^{\ 2}, \tag{1.2}$$

where $\underset{\sim}{p} = (p_r, p_\theta, p_z)$ is the particle momentum in cylindrical coordinates. Consistent with Eq. (1.2), we simply omit the axial self magnetic field $B_z^s(r)$ in the subsequent analysis, since the influence of the axial self magnetic field, produced by the mean rotation $V_\theta^0(r) = \omega_b r$ of the electron beam, on the equilibrium properties is negligibly small in comparison with the influence of azimuthal self magnetic field $B_\theta^s(r)$. A simple estimate gives

$$\left|\frac{V_{\theta b}^0 B_z^s}{V_{zb}^0 B_\theta^s}\right| \simeq \left(\frac{\omega_b a}{V_{zb}^0}\right)^2 \ll 1, \tag{1.3}$$

where $V_{\theta b}^{0}(r)$ is the mean axial velocity of a beam electron fluid element.

Central to a Vlasov description of electron beam equilibria are the single-particle constants of the motion in the equilibrium fields

$$\underset{\sim}{E}^{0}(\underset{\sim}{x}) = E_r^0(r)\,\hat{\underset{\sim}{e}}_r = -\frac{\partial \phi_0(r)}{\partial r}\,\hat{\underset{\sim}{e}}_r \tag{1.4}$$

and

$$\begin{aligned}\underset{\sim}{B}^{0}(\underset{\sim}{x}) &= B_0\,\hat{\underset{\sim}{e}}_z + B_\theta^s(r)\,\hat{\underset{\sim}{e}}_\theta \\ &= B_0\,\hat{\underset{\sim}{e}}_z - \frac{\partial A_z^s(r)}{\partial r}\,\hat{\underset{\sim}{e}}_\theta \end{aligned} \tag{1.5}$$

where $\hat{\underset{\sim}{e}}_r$, $\hat{\underset{\sim}{e}}_\theta$, and $\hat{\underset{\sim}{e}}_z$ are unit vectors in the radial, azimuthal, and axial directions, B_0 is a uniform applied magnetic field, $\phi_0(r)$ is the equilibrium electrostatic potential and $A_z^s(r)$ is the z- component of equilibrium vector potential. For azimuthally symmetric equilibrium with $\partial/\partial z=0$, there are three single particle constants of the motion. These are the total energy H,

$$H = (m^2c^4 + c^2p^2)^{1/2} - e\phi_0(r), \tag{1.6}$$

the canonical angular momentum P_θ

$$P_\theta = r(p_\theta - \frac{1}{2} m\hat{\omega}_{cb} r) \tag{1.7}$$

and the axial canonical momentum

$$P_z = p_z - \frac{e}{c}A_z^s(r) \tag{1.8}$$

where c is the speed of light in *vacuo*, -e and m are charge and rest mass of electron, respectively, and $\hat{\omega}_{cb} = eB_0/mc$ is the nonrelativisitic electron cyclotron frequency in the uniform applied magnetic field B_0. Note that without the applied magnetic field (B_0=0), the term proportional to $\hat{\omega}_{cb}$ in Eq. (1.7) vanishes.

The radial electric field $E_r^0(r)$ and azimuthal self magnetic field $B_\theta^0(r)$ are determined self-consistently from the Maxwell equations

$$\frac{1}{r}\frac{\partial}{\partial r}r\frac{\partial}{\partial r}\phi_0(r) = 4\pi e(1-f_e)n_b^0(r), \tag{1.9}$$

and

$$\frac{1}{r}\frac{\partial}{\partial r}r\frac{\partial}{\partial r}A_z^s(r) = \frac{4\pi e}{c}(1-f_m)n_b^0(r)V_{zb}^0(r), \tag{1.10}$$

where f_e and f_m are the fractional space charge and current neutralizations respectively, of the system [see Eq. (1.1)]. Here, $n_b^0(r)$ and $V_{zb}^0(r)$ are the beam density and axial velocity profiles defined in terms of $f_b^0(H-\omega_b P_\theta, P_z)$ by

$$n_b^0(r) = \int d^3p\ f_b^0(H-\omega_b P_\theta, P_z), \tag{1.11}$$

and

$$n_b^0(r)V_{zb}^0(r) = \int d^3p\ v_z\ f_b^0(H-\omega_b P_\theta, P_z), \tag{1.12}$$

where $v_z = p_z c^2/(m^2c^4+c^2\underset{\sim}{p}^2)^{1/2}$. Equations (1.6) - (1.12) can be used to investigate a wide variety of beam equilibrium properties in the following two sections. Moreover, the mean azimuthal velocity $V_{\theta b}^0(r)$ can also be obtained from

$$n_b^0(r)V_{\theta b}^0(r) = \int d^3p\ v_\theta\ f_b^0(H-\omega_b P_\theta, P_z) \tag{1.13}$$

where $v_\theta = p_\theta c^2/(m^2c^4 + c^2\underset{\sim}{p}^2)^{1/2}$

The organization of this report is the following. In Section 2, we investigate the equilibrium properties of rigid-rotor electron beam with uniform axial drift velocity. The equilibrium distribution function for rigid-rotor electron beam with uniform axial drift velocity is given by

$$f_b^0 = f_b^0(H-\omega_b P_\theta-\beta_b c P_z),$$

which depends on H, P_θ, and P_z exclusively through the linear combination $H-\omega_b P_\theta-\beta_b c P_z$. Here $\beta_b c$ is a constant. The equilibrium properties of a stiff electron beam, which is characterized by zero axial temperature and is described by the distribution function of the form

$$f_b^0 = G(H-\omega_b P_\theta)\,\delta(P_z-\gamma_0 m\beta_0 c),$$

is investigated in Section 3. Here, $G(H-\omega_b P_\theta)$ is an arbitrary function of $H-\omega_b P_\theta$ and $\gamma_0 = (1-\beta_0{}^2)^{-1/2}$ is a constant.

2. ELECTRON BEAM EQUILIBRIA WITH UNIFORM AXIAL DRIFT

We first consider the class of rigid-rotor Vlasov equilibria with uniform axial drifts where f_b^0 depends on H, P_θ and P_z exclusively through the linear combination $H-\omega_b P_\theta-\beta_b cP_z$, where $\beta_b^2=1-1/\gamma_b^2$ =const. That is, we consider beam equilibrium distributions of the form

$$f_b^0 = f_b^0(H-\omega_b P_\theta-\beta_b cP_z)\,. \tag{2.1}$$

We will find that equilibria described by Eq. (2.1) correspond to rigid-rotors with angular velocities ω_b and with uniform axial velocities $V_{zb}^0(r)=\beta_b c$=const. In this regard, it is useful to transform variables in Eq. (2.1) from momentum variables (p_r, p_θ, p_z) appropriate to the laboratory frame to momentum variables (p_r', p_θ', p_z') appropriate to a frame of reference moving with velocity $\beta_b c\,\hat{e}_z$. The relevant transformation is given by

$$p_r=p_r',\, p_\theta=p_\theta',\, p_z=\gamma_b(p_z'+\gamma' m\beta_b c)\,,\, \gamma=\gamma_b(\gamma'+\beta_b p_z'/mc)\,, \tag{2.2}$$

where $\gamma=(1+\underset{\sim}{p}^2/m^2c^2)^{1/2}$ and $\gamma'=(1+\underset{\sim}{p}'^2/m^2c^2)^{1/2}$. After some straightforward algebra with the approximation $\underset{\sim}{p}'^2=(p_r'^2+p_\theta'^2+p_z'^2)\ll m^2c^2$, we find

$$\begin{aligned} &H-\omega_b P_\theta-\beta_b cP_z \\ &= \frac{mc^2}{\gamma_b} + \frac{\underset{\sim}{p}'^2}{2\gamma_b m} - e(\phi_0-\beta_b A_z^s)-\omega_b r(p_\theta'-\gamma_b mr\omega_{cb}/2) \\ &= \frac{mc^2}{\gamma_b} + \frac{1}{2\gamma_b m}[p_r'^2+(p_\theta'-\gamma_b m\omega_b r)^2+p_z'^2]+\hat{\psi}(r)\,, \end{aligned} \tag{2.3}$$

where $\omega_{cb}=\hat{\omega}_{cb}/\gamma_b=eB_0/\gamma_b mc$ is the characteristic electron cyclotron frequency and $\hat{\psi}(r)$ is defined by

$$\begin{aligned} \hat{\psi}(r) &= (1/2)\gamma_b m(\omega_b\omega_{cb}-\omega_b^2)\,r^2-e(\phi_0-\beta_b A_z^s) \\ &= (1/2)\gamma_b m(\omega_b\omega_{cb}-\omega_b^2)\,r^2-e\Phi(r)\,, \end{aligned} \tag{2.4}$$

and $\Phi(r)$ is the effective self-field potential

$$\Phi(r)=\phi_0(r)-\beta_b A_z^s(r). \tag{2.5}$$

In order to evaluate the macroscopic equilibrium properties defined in Eqs. (1.11) - (1.13), it is also necessary to consider the transformation of d^3p to beam frame variables d^3p'. It is straightforward to show from Eq. (2.2) that d^3p transforms according to

$$d^3p=\gamma_b\left(1+\frac{\beta_b p_z'}{\gamma' mc}\right)d^3p'. \tag{2.6}$$

Substituting Eqs. (2.1) - (2.6) into Eq. (1.11), we find that the equilibrium beam density is given by

$$n_b^0(r)=4\pi\gamma_b\int_0^\infty dp''p''^2 f_b^0\left[\frac{mc^2}{\gamma_b}+\frac{p''^2}{2\gamma_b m}+\hat{\psi}(r)\right] \tag{2.7}$$

where the integration variable p'' is defined by

$$p''^2 = p_r'^2+(p_\theta'-\gamma_b m\omega_b r)^2+p_z'^2.$$

Without loss of generality, we assume that the effective self-field potential $\Phi(r)$ vanishes at $r=0$, i.e., $\Phi(r=0)=0$. Similarly the function $\hat{\psi}(r)$ also vanishes at $r=0$. Defining $\hat{n}_b=n_b^0(r=0)$, and

$$F(\hat{\psi}) = \frac{\int_0^\infty dp''p''^2 f_b^0\left(\frac{mc^2}{\gamma_b}+\frac{p''^2}{2\gamma_b m}+\hat{\psi}\right)}{\int_0^\infty dp''p''^2 f_b^0\left(\frac{mc^2}{\gamma_b}+\frac{p''^2}{2\gamma_b m}\right)}, \tag{2.8}$$

Eq. (2.7) can be expressed as

$$n_b^0(r) = \hat{n}_b\, F[\hat{\psi}(r)]. \tag{2.9}$$

It is also straightforward to show from Eqs. (1.12), (2.1) and (2.3) that

$$n_b^0(r)V_{zb}^0(r) = \int d^3p \, \frac{p_z}{\gamma m} \, f_b^0$$

$$= \beta_b c n_b^0(r). \tag{2.10}$$

We note from Eq. (2.10) that $V_{zb}^0(r)$ is uniform over the beam cross section with

$$V_{zb}^0(r) = \beta_b c = \text{const.} \tag{2.11}$$

This is a characteristic property of electron beam equilibria described by an electron distribution function which depends on H and P_z exclusively through the linear combination $H-\beta_b cP_z$. Moreover, substituting Eq. (2.3) into Eqs. (1.13) and (2.1), we readily find

$$V_{\theta b}^0(r) = \omega_b r. \tag{2.12}$$

It is obvious from Eq. (2.12) that the mean aziumthal velocity of the beam electron fluid element is that of a rigid-rotor. Again, this is a typical characteristic of the rigid-rotor beam equilibria in which the distribution function also depends on H and P_θ exclusively through the linear combination of $H-\omega_b P_\theta$. We therefore conclude from Eqs. (2.11) and (2.12) that any electron beam equilibrium described by a distribution which is exclusively a function of $H-\omega_b P_\theta-\beta_b cP_z$, is a rigid-rotor equilibrium distribution with a uniform axial drift.

The remaining important macroscopic quantity that characterizes the electron beam is the equilibrium temperature profile of the beam electrons. The effective beam temperature $T_b^0(r)$ is determined from

$$n_b^0(r)T_b^0(r) = \frac{1}{3}\int d^3p \, [v_r p_r + (v_\theta - V_{\theta b}^0)(p_\theta - \langle p_\theta \rangle)$$

$$+ (v_z - V_{zb}^0)(p_z - \langle p_z \rangle)] \, f_b^0(H-\omega_b P_\theta - \beta_b cP_z) \tag{2.13}$$

where $v_j = p_j c^2/(m^2c^4 + c^2\underset{\sim}{p}^2)^{1/2}$, and $\langle p_j \rangle = (\int d^3p p_j f_b^0)/(\int d^3p f_b^0)$.

Substituting Eq. (2.3) into Eqs. (2.1) and (2.13) gives

$$n_b^0(r)T_b^0(r) = 4\pi\int_0^\infty \frac{dp''}{3m} p''^4 f_b^0\left[\frac{mc^2}{\gamma_b} + \frac{p''^2}{2\gamma_b m} + \hat{\psi}(r)\right], \qquad (2.14)$$

where use has been made of the approximation $p'^2 \ll m^2c^2$. One of the important features in Eq. (2.14) is that the effective beam temperature $T_b^0(r)$ is isotropic, i.e., $T_{rb}^0(r)=T_{\theta b}^0(r)=T_{zb}^0(r)=T_b^0(r)$, where $T_{rb}^0(r)$, $T_{\theta b}^0(r)$, and $T_{zb}^0(r)$ are the effective radial, axiumthal, and axial beam temperatures, respectively, defined by

$$n_b^0(r)T_{jb}^0(r) = \int d^3p \ (v_j - \langle v_j\rangle)(p_j - \langle p_j\rangle) f_b^0 \qquad (2.15)$$

where $\langle v_j\rangle = [\int d^3p(p_j/\gamma m) f_b^0]/(\int d^3p f_b^0)$. Examples of anisotropic beam temperatures will be discussed in the next section.

The Maxwell equation for the effective self-field potential $\Phi(r)$ can be obtained from the linear combination of Eqs. (1.9) and (1.10), and we have

$$\frac{e}{r}\frac{\partial}{\partial r} r \frac{\partial}{\partial r} \Phi(r) = \gamma_b m\omega_{pb}^2 (1-f_e-\beta_b^2+f_m\beta_b^2)F(\hat{\psi}), \qquad (2.16)$$

where $\omega_{pb}^2 = 4\pi\hat{n}_b e^2/\gamma_b m$ is the characteristic plasma frequency-squared and use has been made of Eqs. (2.9) and (2.11). It is evident from Eqs. (1.9), (1.10) and (2.5) that the potentials $\phi_0(r)$ and $A_z^s(r)$ are related to $\Phi=\phi_0-\beta_b A_z^s$ by

$$\phi_0(r) = \frac{1-f_e}{1-f_e-\beta_b^2+f_m\beta_b^2}\Phi(r), \qquad (2.17)$$

and

$$A_z^s(r) = \frac{(1-f_m)\beta_b}{1-f_e-\beta_b^2+f_m\beta_b^2}\Phi(r) \qquad (2.18)$$

Therefore, once the effective potential $\Phi(r)$ is determined from Eq. (2.16) the equilibrium self fields, $E_r^0(r)=-\partial\phi_0/\partial r$ and

$B_\theta^s(r) = -\partial A_z^s/\partial r$, can be calculated self-consistently from Eqs. (2.17) and (2.18).

Eliminating the effective potential $\Phi(r)$ in Eq. (2.16) in favor of the function $\hat{\psi}(r)$ and defining a new dimensionless function

$$\psi(r) = \hat{\psi}(r)/T \ , \tag{2/19}$$

where T = const is a measure of the thermal energy spread for the distribution function f_b^0, we find the nonlinear differential equation for $\psi(r)$:

$$\frac{1}{r}\frac{\partial}{\partial r} r \frac{\partial}{\partial r}\psi(r) = \frac{2\gamma_b m}{T}(\omega_{cb}\omega_b - \omega_b^2)$$

$$- \frac{\gamma_b m \omega_{pb}^2}{T}(1-f_e-\beta_b^2+f_m\beta_b^2)F[\psi(r)]. \tag{2.20}$$

The measure of thermal energy spread T is a parameter characteristic of the beam temperature. Once F is known, the equilibrium problem has been reduced to solving the nonlinear differential equation (2.20) for $\psi(r)$. It is useful to express Eq. (2.20) as

$$\frac{1}{r}\frac{\partial}{\partial r} r \frac{\partial}{\partial r}\psi(r) = \frac{2\gamma_b m}{T}\Big\{(\omega_b^+ - \omega_b)(\omega_b - \omega_b^-)$$

$$+\omega_b^+\omega_b^-[1-F(\psi)]\Big\} , \tag{2.21}$$

where the laminar cold-fluid rotation frequencies $\omega_b^\pm$ are defined by

$$\omega_b^{\pm} = \frac{1}{2}\left[\omega_{cb} \pm (\omega_{cb}^2 - K)^{1/2}\right] , \tag{2.22}$$

in which

$$K = 4\omega_b^+\omega_b^- = 2\omega_{pb}^2(1-f_e-\beta_b^2+f_m\beta_b^2) \tag{2.23}$$

is a measure of the combined strengths of the equilibrium self-electric field $(1-f_e)$ and the equilibrium self-magnetic field $[(1-f_m)\beta_b^2]$.

From the definition of ψ and a careful examination of Eq. (2.21), we find that $\psi(r=0)=0=(\partial\psi/\partial r)_{r=0}$. For physically acceptable solutions of Eq. (2.21) corresponding to radially confined beam equilibria [with $n_b^0(r)$ approaching zero for sufficiently large radius r], $F(\psi)$ is a monotonic decreasing function of increasing ψ with $F(\psi=0)=1$ at $\psi(r=0)=0$, by Eq. (2.8), and $\psi(r)$ is a monotonic increasing function of r. An algebriaic manipulation shows in a straightforward way that

$$\left[\frac{1}{r}\frac{\partial}{\partial r} r \frac{\partial}{\partial r}\psi\right]_{r=0} = \frac{2\gamma_b m}{T}(\omega_b^+ - \omega_b)(\omega_b - \omega_b^-)$$

$$= -(\omega_b - \omega_{cb}/2)^2 + (\omega_{cb}^2 - K)/4 \qquad (2.24)$$

We note from Eq. (2.24) that for a radially confined equilibrium, the beam rotation frequency ω_b is restricted to the range

$$\omega_b^- \leq \omega_b \leq \omega_b^+ , \qquad (2.25)$$

which is only a sufficient condition for radial confinement. The complete necessary and sufficient condition for radially confined equilibrium will be obtained in the specific example. For ω_b in the range of Eq. (2.25), we find $[r^{-1}(\partial/\partial r)(r\partial\psi/\partial r)]_{r=0}>0$. Therefore, beginning with $\psi(0)=0$, if we integrate Eq. (2.21) for small r and ψ, we find that $\psi(r)$ is monotonically increasing near the origin. However, for large r, $\psi(r)$ is not always to be a monotonic increasing function of r. Hence, the inequality in Eq. (2.25) is a sufficient but not necessary condition for a radially confined equilibria.

In Eq. (2.21), ω_b is a variable (as yet unspecified) rotation parameter. Moreover, the nature of the solution for $\psi(r)$ exhibits a strong dependence on the value of ω_b relative to the values of ω_b^+ and ω_b^-, which are the laminar cold-fluid rotation frequencies for a beam with constant density $\hat{n}_b$. For future reference, we plot $\omega_b^\pm$ versus K [Eq. 2.23)] in Figure 2. The segment in the right-half

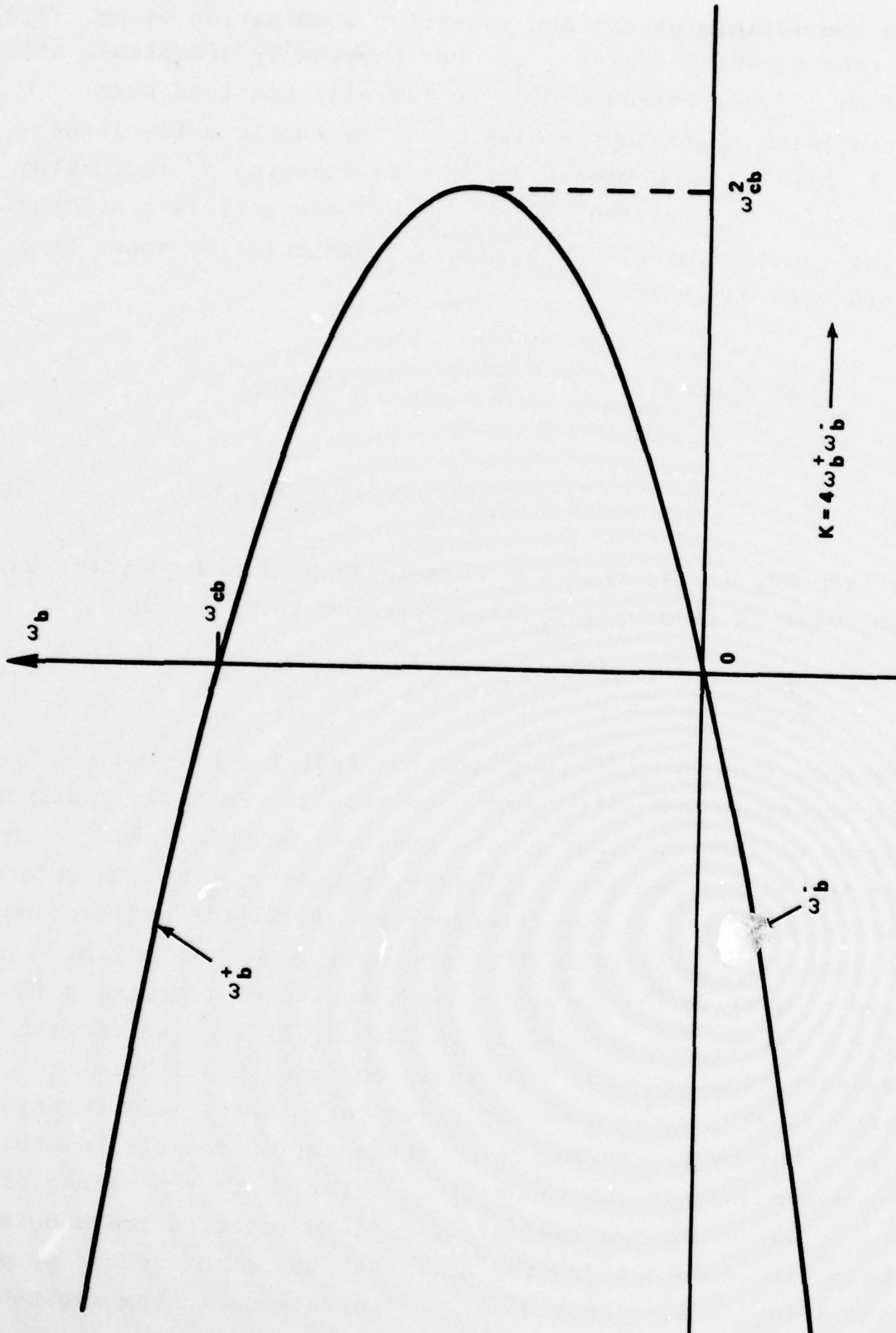

Figure 2. Plot of Laminar Cold-Fluid Rotation Frequencies $\omega_b^{\pm}$ versus $K = 4\omega_b^+\omega_b^-$

plane in Figure 2 corresponds to

$$1-f_e > \beta_b^2(1-f_m) \quad (\text{or } K > 0), \tag{2.26}$$

i.e., the repulsive space-charge force on a beam fluid element exceeds the magnetic focussing force associated with the azimuthal self magnetic field. On the other hand, the left-half plane in Figure 2 corresponds to

$$\beta_b^2(1-f_m) > 1-f_e \quad (\text{or } K < 0), \tag{2.27}$$

in which case the self-magnetic force on a beam fluid element exceeds the repulsive space-charge force. We note from Figure 2 that the $\omega_b^{\pm}$ curves are defined in the entire left-half plane, and converge to the common point $\omega_b^{\pm} = \omega_{cb}/2$ in the right-half plane for a value of beam density satisfying $2\omega_{pb}^2(1-f_e-\beta_b^2+\beta_b f_m) = \omega_{cb}^2$. We also note from Figure 2, and Eqs. (2.22) and (2.24) that no equilibrium solutions exist in the region where

$$K = 2\omega_{pb}^2(1-f_e-\beta_b^2+f_m\beta_b^2)>\omega_{cb}^2. \tag{2.28}$$

The reason is simply that equilibrium space charge force is so strong in this region that the total magnetic attractive forces (self-field plus applied field) cannot overcome the repulsive electrostatic force. Moreover, it is emphasized that without the applied magnetic field, Eq. (2.22) can be further simplified as

$$2\omega_b^{\pm} = (-K)^{1/2} \quad , \tag{2.29}$$

and the $\omega_b^{\pm}$ curves are defined only in the left-half plane of Figure 2.

To complete the general analysis of this equilibrium configuration, we define the effective beam radius a by the relation

$$\hat{n}_b a^2 \equiv 2\int_0^{\infty} dr r n_b^0(r). \tag{2.30}$$

Moreover, we introduce Budker's parameter ν defined by $\nu=N_b(e^2/mc^2)$, where

$$N_b = 2\pi \int_0^\infty drrn_b^0(r) = \pi \hat{n}_b a^2 \qquad (2.31)$$

is the number of electrons per unit axial length of the beam. For a general profile $n_b^0(r)$, we find

$$\frac{\nu}{\gamma_b} = \frac{1}{4} \frac{\omega_{pb}^2 a^2}{c^2} \quad , \qquad (2.32)$$

which is one of the most important parameters in discussing electron beam equilibrium. Evidently, $\nu/\gamma_b \gtrless 1$ accordingly as $a \gtrless 2c/\omega_{pb}$. We now analyze Eq. (2.20) for several specific choices of distribution function f_b^0, which illustrate specifically the qualitative behavior described above.

2.A <u>Sharp - Boundary Beam Equilibria</u>

As a first example, we consider a choice of distribution function for which the beam density is identically zero beyond some radius r_c, i.e., $n_b^0(r>r_c)=0$. In particular, we consider the distribution

$$f_b^0 = \frac{U(T+\frac{mc^2}{\gamma_b} -H+\omega_b P_\theta+\beta_b cP_z)}{(T+\frac{mc^2}{\gamma_b} -H+\omega_b P_\theta+\beta_b cP_z)^{1/2}} \qquad (2.33)$$

where the Heaviside step function U(x) is defined by

$$U(x) = \begin{cases} 1 \ , & x \geq 0 \ , \\ 0 \ , & x < 0 \ . \end{cases} \qquad (2.34)$$

The distribution in Eq. (2.33) is chosen in this subsection simply because the nonlinear differential equation of ψ in Eq. (2.20) becomes linear and can be solved analytically for the entire range of interesting physical parameters. Substituting Eq. (2.33) into Eqs. (2.8) and (2.9), and carrying out the straightforward algebra, we find

$$F(\psi) = [1-\psi(r)] \ U \ (1-\psi) \ , \qquad (2.35)$$

and the electron density profile

$$n_b^0(r) = \hat{n}_b \begin{cases} 1-\psi(r) & , \text{ for } \psi(r)<1, \\ 0 & , \text{ for } \psi(r)>1. \end{cases} \tag{2.36}$$

Before determining the solutions of the nonlinear differential equation of Eq. (2.20), it is convenient to treat separately the cases (a) $1-f_e \geq \beta_b^2(1-f_m)$, and (b) $\beta_b^2(1-f_m)>1-f_e$.

(a) <u>Equilibrium Dominated by Space-Charge Forces</u>

<u>$(1-f_e \geq \beta_b^2 - f_m \beta_m^2)$</u>. We first consider the region of the right-half plane in Figure 2, where

$$0 \leq K = 4\omega_b^+\omega_b^- \leq \omega_{cb}^2. \tag{2.37}$$

In order to reduce the number of independent parameters in Eq. (2.20), we introduce the dimensionless variable

$$X = r/d_0 \ , \tag{2.38}$$

where d_0 is defined by

$$d_0^2 = 16T/\gamma_b mK \ . \tag{2.39}$$

Substituting Eq. (2.35) into Eq. (2.20), and making use of Eqs. (2.38) and (2.39) gives

$$\frac{1}{X}\frac{\partial}{\partial X} X \frac{\partial}{\partial X}\psi = 8\zeta - \begin{cases} 8(1-\psi) & , 0<r<r_c \ , \\ 0 & , r>r_c \ , \end{cases} \tag{2.40}$$

where

$$\zeta = 4\omega_b(\omega_{cb}-\omega_b)/K \ , \tag{2.41}$$

and r_c is the confinement radius satisfying $\psi(r_c)=1$. For $r<r_c$, the solution to Eq. (2.40) is

$$\psi(X) = (\zeta-1)[I_0(2\sqrt{2}X)-1] \ , \tag{2.42}$$

where $I_0(x)$ is the modified Bessel function of the first kind of order zero. In obtaining Eq. (2.42), use has been made of $\psi(r=0)=0$ [see the discussion following Eq. (2.23)].

Since the function $\psi(r)$ must be greater than zero for all r, it is quite obvious from Eq. (2.42) that

$$\zeta > 1 \tag{2.43}$$

is the necessary and sufficient condition in the case for a radially confined beam equilibrium. [Note that $I_0(\infty) = \infty$.]. Making use of the definition of ζ in Eq. (2.41), Eq. (2.43) can be expressed as Eq. (2.25) for a positive value K. Thus, we conclude from Eq. (2.43) that the space-charge dominated electron beam described by Eq. (2.33) is in radially confined equilibria provided the beam rotation frequency ω_b is in the range $\omega_b^- < \omega_b < \omega_b^+$. Substituting Eq. (2.42) into Eq. (2.36), we find the electron density profile

$$n_b^0(r) = \hat{n}_b \begin{cases} \zeta-(\zeta-1)\ I_0(2\sqrt{2}X), & 0<r<r_c\ , \\ 0 & , \ r>r_c\ , \end{cases} \tag{2.44}$$

where the beam confinement radius r_c is obtained from

$$I_0(2\sqrt{2}r_c/d_0) = \zeta/(\zeta-1). \tag{2.45}$$

The effective beam radius a defined in Eq. (2.30) can be simply expressed as

$$a^2 = \zeta r_c^2 - (\sqrt{2}/2)(\zeta-1)r_c d_0 I_1(2\sqrt{2}r_c/d_0) \tag{2.46}$$

In Eq. (2.46) $I_1(x)$ is the modified Bessel function of order one. Note from Eqs. (2.45) and (2.46) that the beam confinement radius r_c and the effective beam radius a increase to infinity when ζ approaches unity. Moreover, the measure of the thermal energy spread T plays a significant role in determining the confinement radius r_c and beam radius a [see Eqs. (2.39), (2.45) and (2.46)].

(b) <u>Equilibrium Dominated by Self-Magnetic Forces</u> <u>($\beta_b^2 - f_m\beta_b^2 > 1-f_e$)</u>. We now consider the left-half plane in Figure 2, where

$$K = 4\omega_b^+\omega_b^- < 0 \ . \tag{2.47}$$

In this region, $\beta_b^2 - f_m\beta_b^2 > 1-f_e$, i.e., the self-magnetic force on a beam fluid element exceeds the repulsive space-charge force. It is convenient to analyze Eq. (2.20) with the radial variable r normalized in units of the Bennett pinch radius b_0 [see Eq. (2.83)]. Defining

$$X'' = r/b_0, \tag{2.48}$$

where

$$b_0^2 = - d_0^2 = 16T/\gamma_b m|K|, \tag{2.49}$$

Eq. (2.20) can be expressed in the form

$$\frac{1}{X''}\frac{\partial}{\partial X''} X'' \frac{\partial}{\partial X''} \psi = -8\zeta + \begin{cases} 8(1-\psi), & 0<r<r_c \ , \\ 0 & , \ r<r_c \ , \end{cases} \tag{2.50}$$

where ζ is again defined in Eq. (2.41). For $r<r_c$, the solution $\psi(X'')$ that satisfies $\psi(X''=0)=0$ is given by

$$\psi(X'')=(1-\zeta)[1-J_0(2\sqrt{2}X'')] \ , \tag{2.51}$$

where $J_0(x)$ is the Bessel function of the first kind of order zero. Once again, in order to have a positive $\psi(r)$ for all r, it is necessary that

$$\zeta < 1 \ , \tag{2.52}$$

which also can be expressed, as in Eq. (2.25), as $\omega_b^- < \omega_b < \omega_b^+$ for a negative K value. In this case, the inequality in Eq. (2.25) is only a sufficient condition for radially confined equilibrium.

However, Eq. (2.25) is not a necessary condition for radial confinement, since the function $\psi(r)$ in Eq. (2.51) is always smaller than unity for a certain range of the physical parameter ζ even if ζ satisfies Eq. (2.52). In order to have radially confined equilibrium, the value of the function $\psi(r)$ must be greater than unity for $r > r_c$, where r_c satisfies $\psi(r_c)=1$. In finding a necessary condition for radial confinement, it is important to investigate the properties of Eq. (2.50) and the Bessel function $J_o(x)$ which has the minimum value $J_o(\alpha_{01}) \simeq -0.402$ at $x=\alpha_{01}$. Here $\alpha_{01}=3.83$ is the first root of $J_1(\alpha_{01})=0$ and $J_1(x)$ is the Bessel function of order one. Since the value of $\psi(r)$ is always greater than unity for $r > r_c$ when $\zeta > 0$ [Examine carefully Eq. (2.50)], we find the necessary and sufficient condition

$$0 < \omega_b < \omega_{cb} \tag{2.53}$$

for a radially confined equilibrium.

The equilibrium properties of the electron beam corresponding to

$$0 < \zeta \le 1 - [1-J_o(\alpha_{01})]^{-1} \tag{2.54}$$

where the right-hand side inequality is obtained from $\psi(\alpha_{01}/2\sqrt{2}) \ge 1$, are also very interesting. In terms of the beam rotation frequency ω_b, Eq. (2.54) can be expressed as

$$\hat{\omega}_b^- < \omega_b < 0 \text{ or } \omega_{cb} < \omega_b < \hat{\omega}_b^+ \tag{2.55}$$

where $\hat{\omega}_b^{\pm}$ is determined by

$$\hat{\omega}_b^{\pm} = \frac{1}{2}\left(\omega_{cb} \pm \left\{\omega_{cb}^2 - K + K[1-J_0(\alpha_{01})]^{-1}\right\}^{1/2}\right)$$

In this case, the value of the function $\psi(r)$ would be less than unity for several subranges of r. Thus, the density profile would have subsidiary peaks at successive radii and the central beam would be surrounded by coaxial cylindrical beams for ζ in the range $0 < \zeta \le [1-J_0(\alpha_{01})]^{-1}$. The physical significance of such a configuration is not yet clear. We shall call this condition the <u>multi annular beam</u> equilibrium.

Substituting Eq. (2.51) into Eq. (2.30), we find the density profile of beam electrons

$$n_b^0(r) = \hat{n}_b[\zeta+(1-\zeta)J_0(2\sqrt{2}r/b_0)], \tag{2.56}$$

for either radially confined or oscillatory equilibrium. For a radially confined equilibrium, in which the beam rotation frequency ω_b satisfies Eq. (2.53), the beam density becomes zero at the radial confinement radius r_c. On the other hand, if ω_b is in the range

$$\hat{\omega}_b^+ < \omega_b < \omega_b^+ \quad \text{or} \quad \omega_b^- < \omega_b < \hat{\omega}_b^-, \tag{2.57}$$

we find from Eq. (2.51) that $\psi(r)$ [and hence $n_b^0(r)$] exhibits oscillatory behavior with its maximum value always less than unity. Evidently from Eq. (2.56), in this oscillatory equilibrium, the beam density $n_b^0(r)$] decreases from $\hat{n}_b$ at r=0, to $\zeta\hat{n}_b$ as $r\to\infty$. Moreover, the beam density exhibits an oscillatory dependence on r, with characteristic radial wave number

$$k_r = \frac{2\sqrt{2}}{b_0} = \frac{1}{2}\left(\frac{2\gamma_b m|K|}{T}\right)^{1/2}, \tag{2.58}$$

where b_0 is the Bennett pinch radius.

The effective beam radius a is estimated by substitution of Eq. (2.56) into Eq. (2.30) and we find

$$a^2 = \zeta r_c^2+(\sqrt{2}/2)(1-\zeta)r_c b_0 J_1(2\sqrt{2}r_c/b_0), \tag{2.59}$$

where the radial confinement radius r_c is obtained from

$$J_0(2\sqrt{2}r_c/b_0) = \zeta/(\zeta-1). \tag{2.60}$$

When the self-magnetic force exceeds the repulsive space-charge force, the maximum radial confinement radius r_{cm} of the electron beam described by Eq. (2.33) is given by

$$r_{cm} = \alpha_{01}b_0/2\sqrt{2}, \tag{2.61}$$

which corresponds to $\zeta = 1 - [1-J_0(\alpha_{01})]^{-1}$. Moreover, the radial confinement radius r_c (hence the effective beam radius a) increases by increasing the mesaure of thermal energy spread T [see Eqs. (2.49), (2.59) and (2.60)].

A summary of the equilibrium properties for the electron beam described by Eq. (2.33) is presented in Figure 3. Figure 3 is similar to Figure 2 except for the addition of a plot of $\hat{\omega}_b^+$ versus $K = 4\omega_b^+\omega_b^-$ in the left-half plane where the self-magnetic force exceeds the replusive space-charge force. We reiterate that for an electron beam dominated by space-charge force $(1-f_e > \beta_b^2 - f_m\beta_b^2)$, both <u>necessary and sufficient</u> condition for a radially contined equilibrium is given by Eq. (2.25). On the other hand, Eq. (2.53) is the <u>necessary and sufficient</u> condition for a radially confined beam equilibrium dominated by a self-magnetic force$(\beta_b^2 - f_m\beta_b^2 > 1-f_e)$. These are illustrated by the cross-hatched region in Figure 3.

Finally, we calculate the beam temperature profile defined in Eq. (2.14). Substituting Eq. (2.33) into Eq. (2.7) and (2.14), it is straightforward to show that

$$T_b^0(r) = \frac{1}{2}T[1-\psi(r)], \tag{2.62}$$

which decreases from T/2 at r=0, to zero at $r=r_c$ for a radially confined equilibrium. Evidently, the measure of thermal energy spread T is directly related to the beam temperature. We therefore conclude from Eqs. (2.46), (2.49) and (2.59) that the effective beam radius a increases considerably when the beam temperature is increased.

2.B <u>Diffuse Beam Equilibrium - The Generalized Bennett Pinch</u>

As a second example, we consider the choice of distribution function

$$f_b^0(H, P_\theta, P_z) = \frac{1}{Z_b}\exp[-(H-\omega_b P_\theta - \beta_b c P_z)/T], \tag{2.63}$$

where the normalization constant Z_b^{-1} is defined by

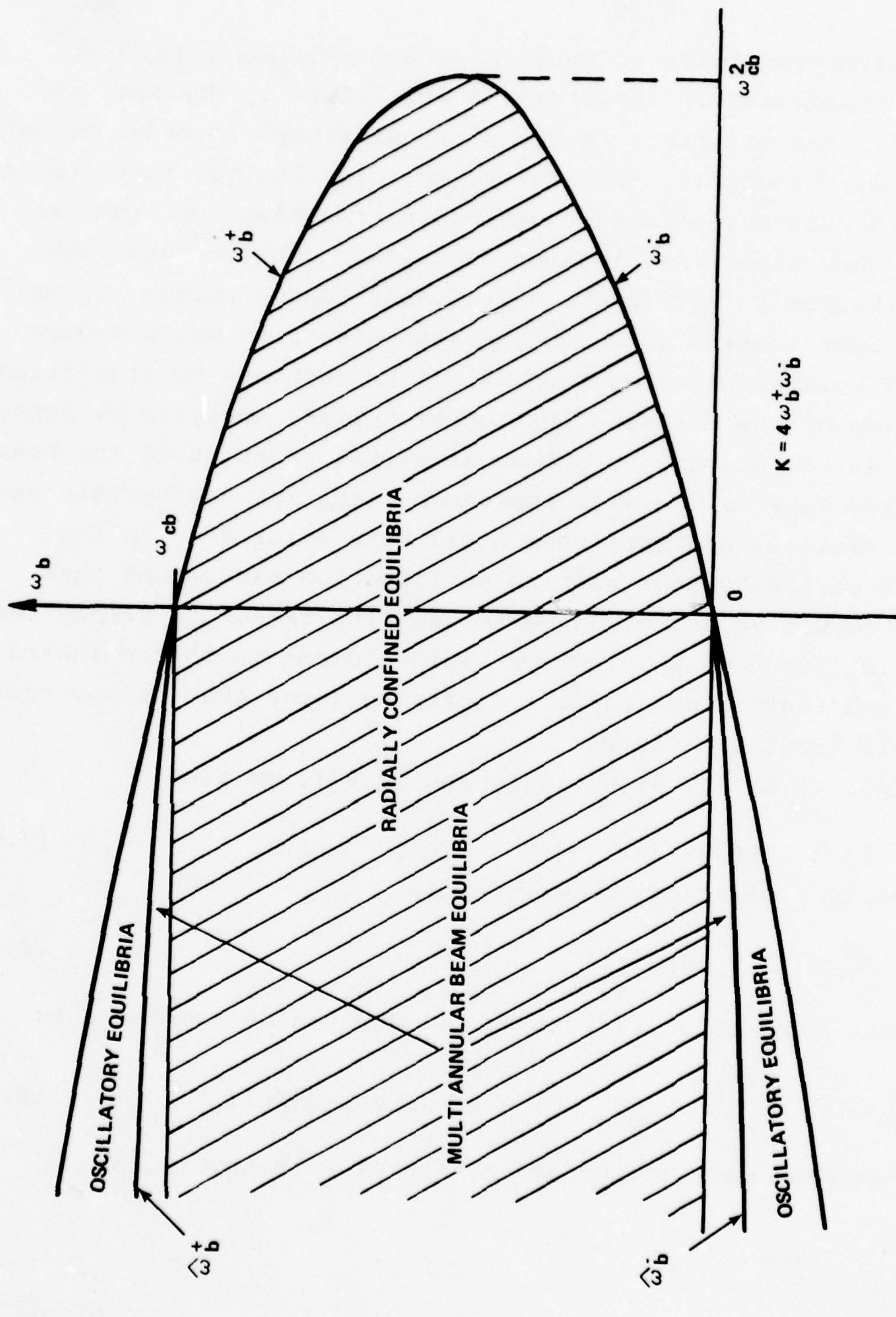

Figure 3. Radially Confined Equilibrium Boundaries for Electron Beam Described by Eq. (2.33).

$$z_b^{-1} = \frac{\hat{n}_b}{\gamma_b} \frac{1}{(2\pi\gamma_b mT)^{3/2}} \exp(mc^2/\gamma_b T). \tag{2.64}$$

The equilibrium properties of the electron beam described by Eq.(2.63) have been investigated in the previous literature[5]. However, we repeat some of the arguments in the previous study[5] in order to make this report more complete. Moverover, the distribution function in Eq. (2.63) is used more often in describing the electron beam properties than any other distribution function, mostly because the Gibbs distribution in Eq. (2.63) corresponds to the unique thermal equilibrium distribution to which the beam electrons would evolve through self collisions. Equation (2.63) corresponds to significant generalization of the distribution function first analyzed by Bennett[2] in that Eq. (2.63) allows for a mean azimuthal rotation of the beam electrons when ($\omega_b \neq 0$). We will therefore find, for appropriate choice of ω_b, that radially confined beam equilibria exist even in the absence of a partially neutralizing positive ion background that weakens the repulsive space charge force. The reason is simply that the $\omega_b r \hat{e}_\theta \times B_0 \hat{e}_z$ force on an electron fluid element is in the inward direction, and therefore acts as a confining force that can overcome repulsive electrostatic forces.

From Eqs. (2.8), (2.9), (2.19), and (2.63), we find

$$F(\psi) = \exp[-\psi(r)] \tag{2.65}$$

and the density profile of the beam electron

$$n_b^0(r) = \hat{n}_b \exp[-\psi(r)] \tag{2.66}$$

The nonlinear equation of $\psi(r)$ in Eq. (2.20) can be expressed as

$$\frac{1}{r}\frac{\partial}{\partial r} r \frac{\partial}{\partial r}\psi(r) = \frac{2\gamma_b m}{T}(\omega_{cb}\omega_b - \omega_b^2) - \frac{\gamma_b m}{2T} K \exp[-\psi(r)], \tag{2.67}$$

where use has been made of the definition of K in Eq. (2.23).

(a) Necessary and Sufficient Conditions for Radially Confined Equilibrium

We now make use of Eqs. (2.21) and (2.65) for $\psi(r)$, together with the definitions in Eqs. (2.22) and (2.23), to determine the necessary and sufficient conditions for radially confined equilibria, i.e., equilibria characterized by

$$\lim_{r\to\infty} n_b^0(r) = \lim_{r\to\infty} \hat{n}_b \exp[-\psi(r)] = 0$$

or equivalently

$$\lim_{r\to\infty} \psi(r) = +\infty.$$

In this regard, we investigate properties of the solution to Eq. (2.21), subject to the boundary conditions $\psi(r=0)=0$ and $\psi(r\to\infty)=\infty$. Evidently, if $\psi(r)$ is a monotonic increasing function of r, then $n_b^0(r)=\hat{n}_b\exp(\psi)$ is a monotonic decreasing function of r, decreasing from $\hat{n}_b$ at r=0 to zero as $r\to\infty$. Since the sufficient condition for radial confinement has been already obtained in Eq. (2.25) for general rigid-rotor equilibria, we investigate here the necessary condition for radial confinement particularly for the Gibbs distribution function in Eq. (2.63).

Equilibrium Dominated by Space-Charge Forces $(1-f_e \geq \beta_b^2 - \beta_b^2 f_m)$.
We first consider the region of the right-half plane in Figure 4 where $K>0$. To show that Eq. (2.25) is also a necessary condition for a radially confined equilibrium, let us assume that ω_b is outside the range in Eq. (2.25) (either $\omega_b>\omega_b^+$ or $\omega_b<\omega_b^-$) and that $\psi(r\to\infty)=\infty$, which corresponds to $n_b^0(r\to\infty)=0$. This will lead to a contradiction. For $\omega_b>\omega_b^+$ or $\omega_b<\omega_b^-$, we conclude from Eq. (2.24) that $[r^{-1}(\partial/\partial r)(r\partial\psi/\partial r)]_{r=0}<0$, so that $\psi(r)$ decreases to negative values near the origin. If $\psi(r)$ is to eventually assume a positive value so that $\psi(r\to\infty)=\infty$, then $\psi(r)$ must pass through a minimum (Figure 5) at $r=r_1$, say, where $\psi(r_1)<0$, $(\partial\psi/\partial r)_{r=r_1}=0$ and $(\partial^2\psi/\partial r^2)_{r=r_1}>0$. Evaluating Eq. (2.21) at $r=r_1$, we find

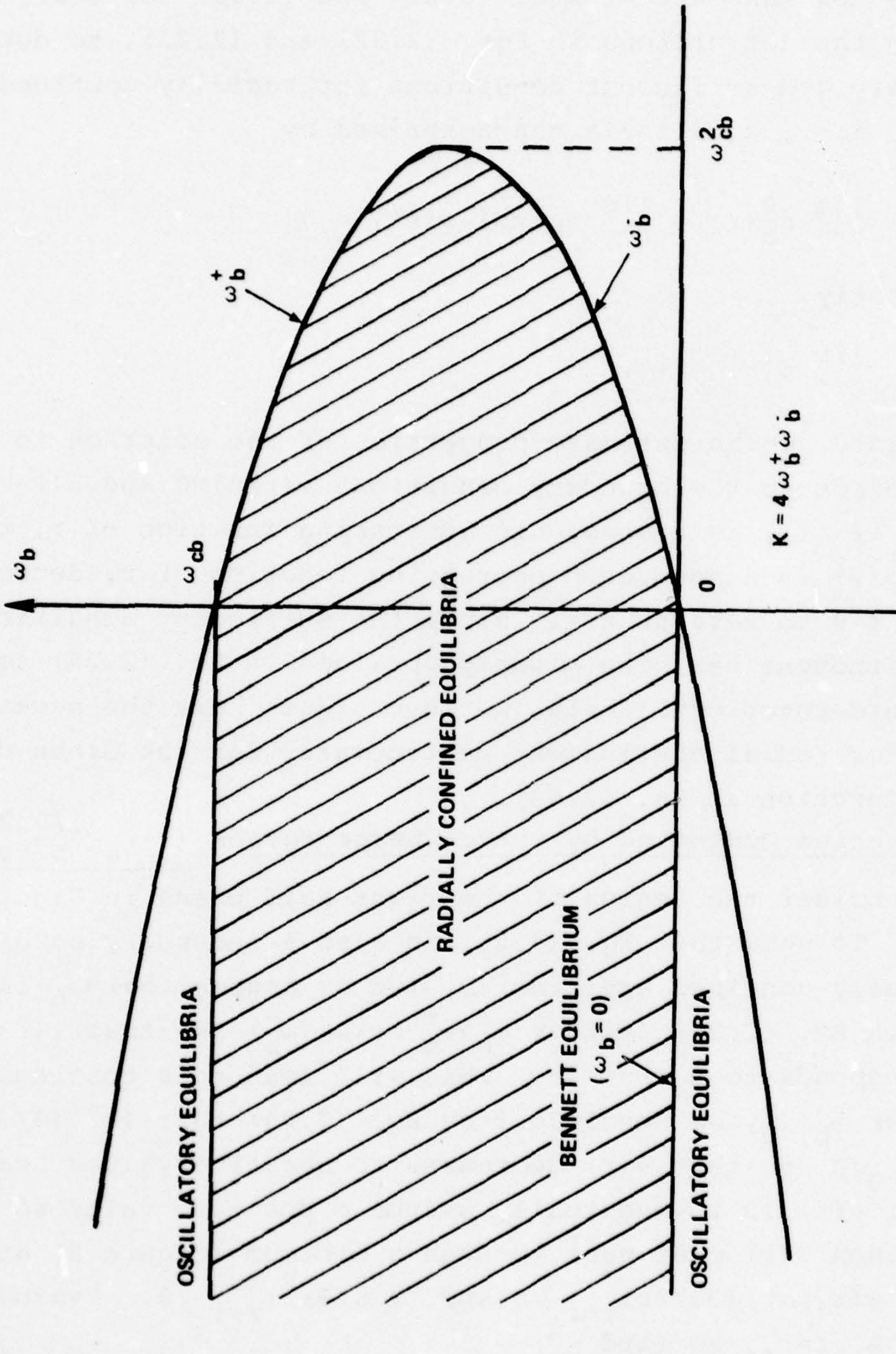

Figure 4. Radially Confined Equilibrium Boundaries for Electron Beam Described by Eq. (2.63)

$$\left(\frac{\partial^2\psi}{\partial r^2}\right)_{r=r_1} = \frac{2\gamma_b m}{T}\left\{(\omega_b^+-\omega_b)(\omega_b-\omega_b^-)+\omega_b^+\omega_b^-[1-\exp(-\psi)]\right\}, \tag{2.68}$$

which is manifestly negative for $\psi(r_1)<0$ and ω_b satisfying $\omega_b>\omega_b^+$ or $\omega_b<\omega_b^-$. [Keep in mind $K=4\omega_b^+\omega_b^-\geq 0$]. We therefore conclude that $\omega_b>\omega_b^+$ or $\omega_b<\omega_b^-$ is contradictory to the assumption of a radially confined equilibrium with $\psi(r\to\infty)=+\infty$. Hence, a restriction of the rotational parameter ω_b to the range specified by Eq. (2.25) is both necessary and sufficient for a radially confined equilibrium dominated by space charge force. This is illustrated by the cross-hatched region in the right-half plane of Figure 4.

Equilibrium Dominated by Self-Magnetic Forces $(\beta_b^2-f_m\beta_b^2>1-f_e)$.

We now consider the left-half plane in Figure 4 where $K=4\omega_b^+\omega_b^-<0$. A determination of the necessary and sufficient conditions for radially confined equilibrium solutions when $K<0$ (Figure 4) proceeds in a similar manner to the analysis in the case $K>0$. We therefore summarize the essential results. For $K=4\omega_b^+\omega_b^-<0$, a restriction of the rotational parameter ω_b to the range

$$0\leq\omega_b\leq\omega_{cb} \tag{2.69}$$

is both necessary and sufficient for the solution to Eq. (2.67) to correspond to a radially confined equilibrium characterized by $n_b^0(r\to\infty)=0$ and $\psi(r\to\infty)=+\infty$. This range is illustrated by the cross-hatched region in the left-half plane of Figure 4. Moreover, for $K<0$ and $0\leq\omega_b\leq 1$, the beam density profile $n_b^0(r)$ is a monotonic decreasing function of r. Finally, for $K<0$, if ω_b is in the range

$$\omega_{cb}<\omega_b<\omega_b^+ \text{ or } \omega_b^-<\omega_b<0, \tag{2.70}$$

we find from Eq. (2.67) that $\psi(r)$ [and hence $n_b^0(r)$] exhibits oscillatory behavior.

To summarize the results, we find that radially confined equilibrium solutions exist provided $-\infty<K=4\omega_b^+\omega_b^-<1$ and ω_b lies in the cross-hatched region in Figure 4. Moreover, for $\beta_b^2 - f_m\beta_b^2 > 1 - f_e$, and $\hat{\omega}_b$ in the range $\omega_{cb} < \omega_b < \omega_b^+$ or $\omega_b^- < \omega_b < 0$, the density profile $n_b^0(r)$, although a nonincreasing function of r on the average, does exhibit an oscillatory radial dependence. Furthermore, we note from Eq. (2.67) that if $\omega_b = \omega_b^+$ or $\omega_b = \omega_b^-$, then the solution to Eq. (2.67) is $\psi(r) = 0$, which corresponds to uniform beam density for all r.

(b) Exact Analytic Solutions

Equation (2.67) does permit exact analytic solutions for certain special choices of the rotational parameter ω_b, or the quantity $K = 4\omega_b^+\omega_b^-$ that measures the strength of the equilibrium self fields. Before determining these solutions, we find from Eq. (2.13) that the beam temperature profile for the Gibbs distribution function is given by the isothermal value

$$T_b^0(r) = T = \text{const.} \tag{2.71}$$

We now determine the exact solution to Eq. (2.67) for two special choices of equilibrium parameters: (a) $1 - f_e = \beta_b^2 - f_m\beta_b^2$, which corresponds to a self-field force-free equilibrium, and (b) $\omega_b(\omega_{cb} - \omega_b) = 0$, which corresponds to an equilibrium in which the magnetic force associated with the applied field and the centrifugal force exactly cancel.

Self-Field Force-Free Equilibrium. In the special case where

$$K = 4\omega_b^+\omega_b^- = 2\omega_{pb}^2(1 - f_e - \beta_b^2 + f_m\beta_b^2) = 0, \tag{2.72}$$

i.e., the magnetic and electric self-field force on a beam fluid element exactly cancel, Eq. (2.67) reduces to the simple linear equation

$$\frac{1}{r}\frac{\partial}{\partial r}r\frac{\partial}{\partial r}\psi(r) = \frac{2\gamma_b m}{T}(\omega_{cb}\omega_b - \omega_b^2). \tag{2.73}$$

The solution to Eq. (2.73) is

$$\psi(r) = r^2/a_0^2, \tag{2.74}$$

where

$$a_0^2 = \frac{(2T/\gamma_b m)}{\omega_b(\omega_{cb}-\omega_b)} \tag{2.75}$$

Moreover, the density profile $n_b^0(r)=\hat{n}_b \exp(-\psi)$ is given by the Gaussian profile

$$n_b^0(r) = \hat{n}_b \exp\left\{-r^2/a_0^2\right\} . \tag{2.76}$$

The effective beam radius a is found by

$$a = a_0 \tag{2.77}$$

from Eq. (2.30) for the self-field force-free equilibrium. Note that K=0 [Eq. (2.72)] corresponds to the vertical axis in Figure 4 and $0<\omega_b<\omega_{cb}$ is required [Eq. (2.75)] in order for the beam equilibrium to be radially confined with $a_0^2>0$.

Equilibrium With $\omega_b(\omega_{cb}-\omega_b)=0$. As a second example that has an exact analytic solution, we consider the case where the centrifugal and applied magnetic forces exactly cancel, i.e., $\omega_b(\omega_{cb}-\omega_b)$, or equivalently

$$\omega_b=0 \quad \text{or} \quad \omega_b=\omega_{cb} . \tag{2.78}$$

From Figure 4 and Eq. (2.69), we therefore require $\beta_b^2-f_m\beta_b^2>1-f_e$ for radially confined equilibrium solutions. Making use of Eq. (2.78), we find that Eq. (2.67) can be expressed as

$$\frac{1}{r}\frac{\partial}{\partial r} r \frac{\partial}{\partial r}\psi(r) = \frac{8}{b_0^2} \exp\left\{-\psi(r)\right\} , \tag{2.79}$$

where

$$b_0^2 = \frac{16T}{\gamma_b m|K|} = \frac{8T/\gamma_b m}{\omega_{pb}^2(\beta_b^2-f_m\beta_b^2-1+f_e)} . \tag{2.80}$$

The solution to Eq. (2.79) is given by

$$\psi(r) = 2\ell n(1+r^2/b_0^2), \tag{2.81}$$

and the beam density profile $n_b^0(r) = \hat{n}_b \exp(-\psi)$ reduces to

$$n_b^0(r) = \frac{\hat{n}_b}{(1+r^2/b_0^2)^2} \quad , \tag{2.82}$$

which is identical to that obtained by Bennett[2]. Substituting Eq. (2.82) into Eq. (2.30), we find the Bennett pinch radius

$$a = b_0, \tag{2.83}$$

which has been introduced into Eq. (2.48). The equilibrium self fields can be calculated from Eqs. (2.4), (2.17), (2.18), (2.19) and (2.81). We find

$$E_r^0(r) = -\frac{\gamma_b m}{2e}\,\omega_{pb}^2(1-f_e)\frac{r}{1+r^2/b_0^2} \tag{2.84}$$

and

$$B_\theta^s(r) = -\frac{\gamma_b m}{2e}\,\omega_{pb}^2\beta_b(1-f_m)\frac{r}{1+r^2/b_0^2} \quad . \tag{2.85}$$

We note from Eq. (2.80) that the effective beam radius $a=b_0$ becomes large whenever $\beta_b^2(1-f_m)$ is closely tuned to $1-f_e$, i.e., whenever the self-magnetic pinching force almost cancels the repulsive electrostatic force.

(c) Numerical Solutions to Eq. (2.67)

The exact analytic solution to Eq. (2.67) is accessible only in certain special limiting cases [see Eqs. (2.74) and (2.81)]. Here we solve Eq. (2.67) numerically for a variety of system parameters of experimental interest. To reduce the number of independent parameters, we introduce the dimensionless variable

$$X' = r/a_0 \quad , \tag{2.86}$$

where a_0 is the effective beam radius defined for self-field force-free equilibrium (2.75). Making use of Eq. (2.86), Eq. (2.67) reduces to

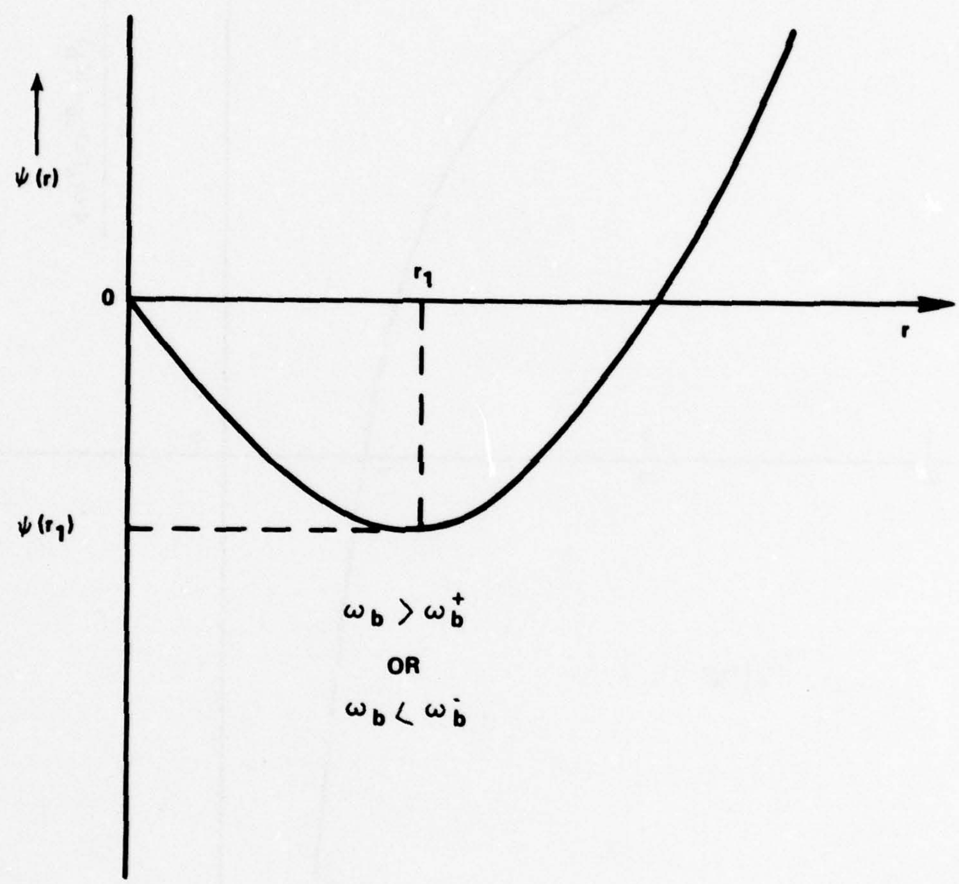

Figure 5. Plot of $\psi(r)$ versus r for $\omega_b > \omega_b^+$ or $\omega_b < \omega_b^-$ and radial confinement.

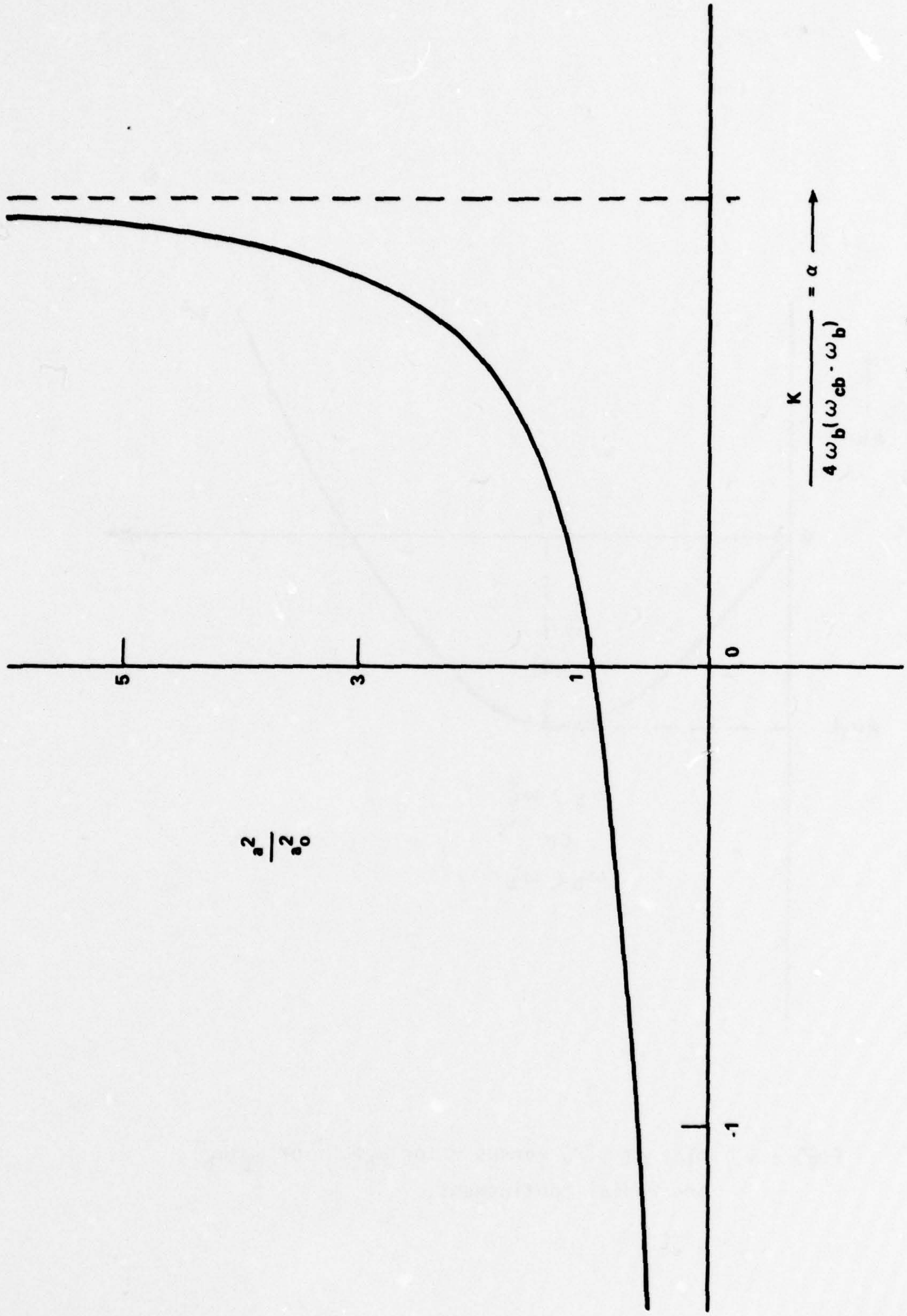

Figure 6. Plot of Normalized Effective Beam Radius-squared a^2/a_0^2 versus Parameter α in Eq. (2.89) for Diffused Beam Equilibrium

$$\frac{1}{X'}\frac{\partial}{\partial X'}X'\frac{\partial}{\partial X'}\psi = 4[1-\alpha \exp(-\psi)] , \tag{2.87}$$

where α is defined by

$$\alpha = \frac{K}{4\omega_b(\omega_{cb}-\omega_b)} . \tag{2.88}$$

Figure 6 shows a plot of the normalized effective beam radius-squared defined by

$$\frac{a^2}{a_0^2} = 2\int_0^\infty dX'X' \exp\left\{-\psi(X')\right\} \tag{2.89}$$

versus α [Eq. (2.88)], which is a measure of the beam density and self-field strength. Note from Figure 6 that the effective beam radius a increases monotonically from a_0 when $\alpha=0$, to infinity when $\alpha=1$, or equivalently $\omega_b=\omega_b^+$ or $\omega_b=\omega_b^-$. Moreover, for $\alpha<0$ (i.e., $\beta_b^2-f_m\beta_b^2>1-f_e$), a decreases from $a=a_0$ when $\alpha=0$, to zero when α tends to minus infinity. Equation (2.87) has been solved numerically for various choices of α. This is illustrated in Figures 7 and 8, where $\psi(X')$ is plotted versus $X'=r/a_0$ (Figure 7), and the corresponding normalized density profile $n_b^0(X')/\hat{n}_b=\exp[-\psi(X')]$ is plotted versus $X'=r/a_0$ (Figure 8) for several values of α. We emphasize from the definition of a_0 in Eq. (2.75) that the numerical analysis of Eq. (2.87) is valid only when the beam rotational parameter ω_b is in the range $0<\omega_b<\omega_{cb}$. Note from Figure 7 that $\psi(X')$ is a monotonic increasing function of X' for each value of α. Moreover, for specified X', $\psi(X')$ decreases as α increases, with $\psi(X')=0$ in the limit where $\alpha=1$. We also note from Figure 8 that the curve for $\alpha=0$ corresponds to the gaussian density profile in Eq. (2.76).

In the region where the self-magnetic focussing force exceeds the electrostatic repulsive force, i.e., $K<0$, it is convenient to analyze Eq. (2.67) with radial variable r normalized in units of the Bennett pinch radius b_0 derived for $\omega_b(\omega_{cb}-\omega_b)=0$ [Eq. (2.83)]. Defining

$$X''=r/b_0 , \tag{2.90}$$

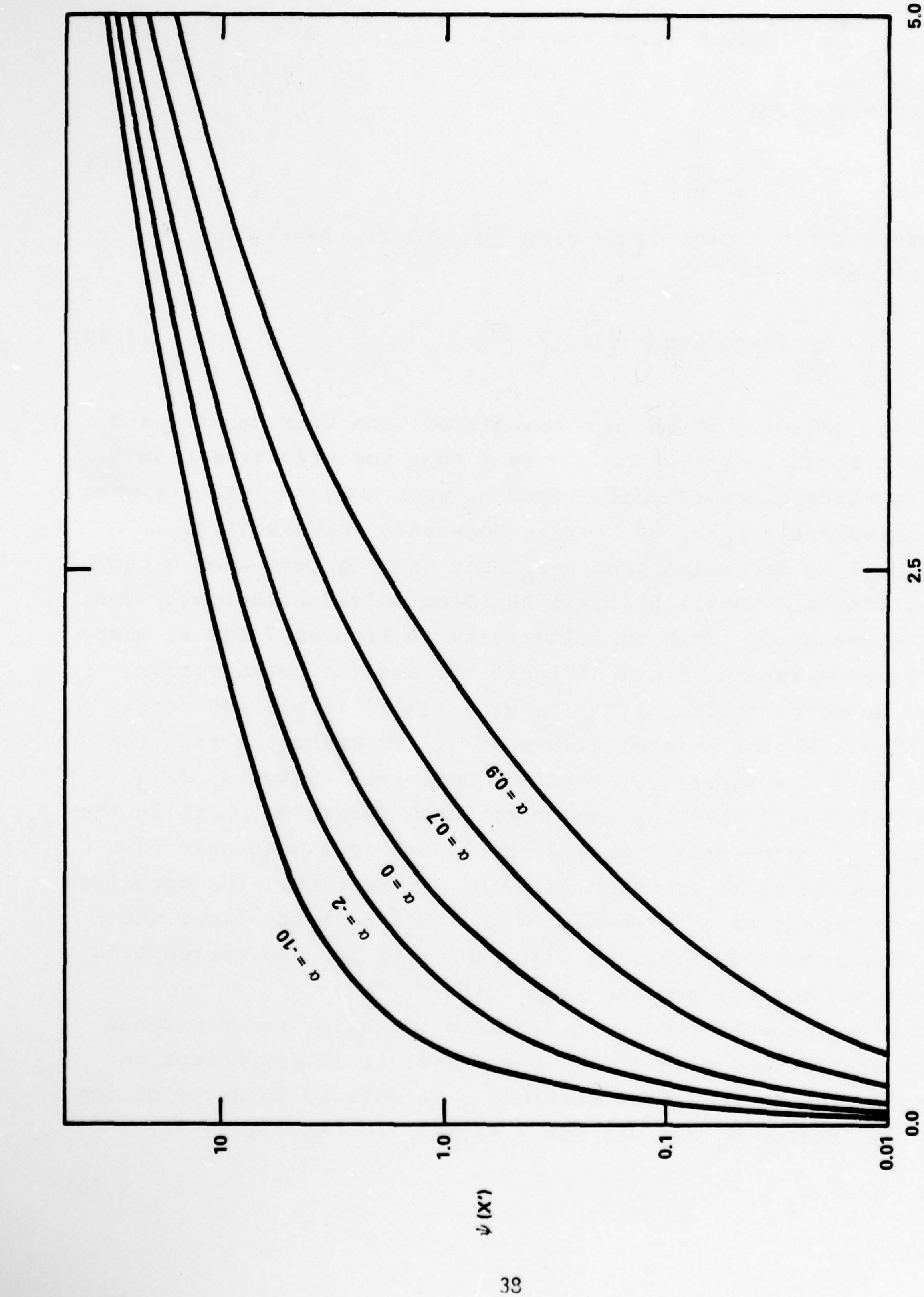

Figure 7. Plot of $\psi(x')$ versus x Eq. (2.87) for Several Values of α

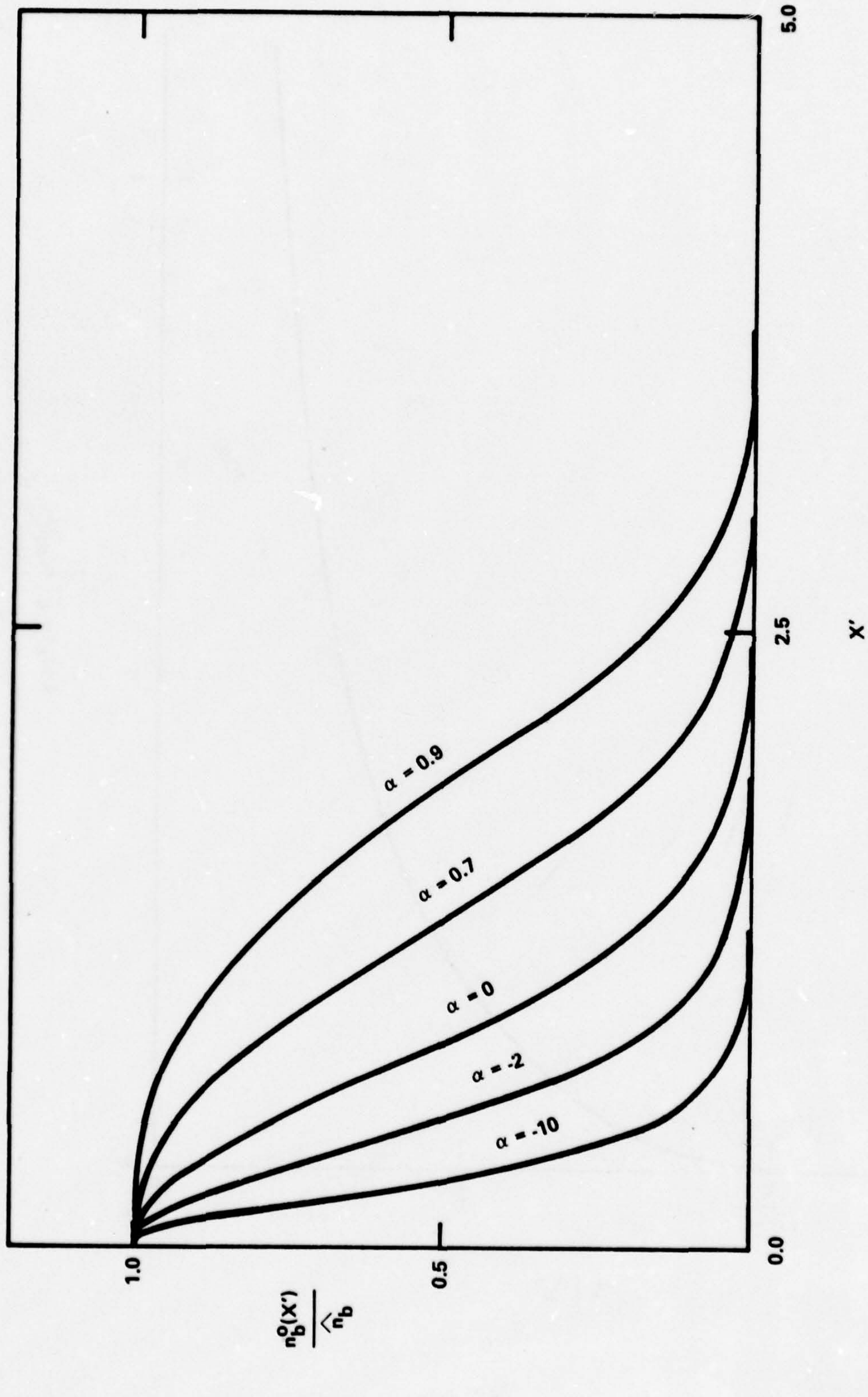

Figure 8. Plot of Normalized Beam Electron Density versus x'[Eqs. (2.66) and (2.87)] for Several values of α.

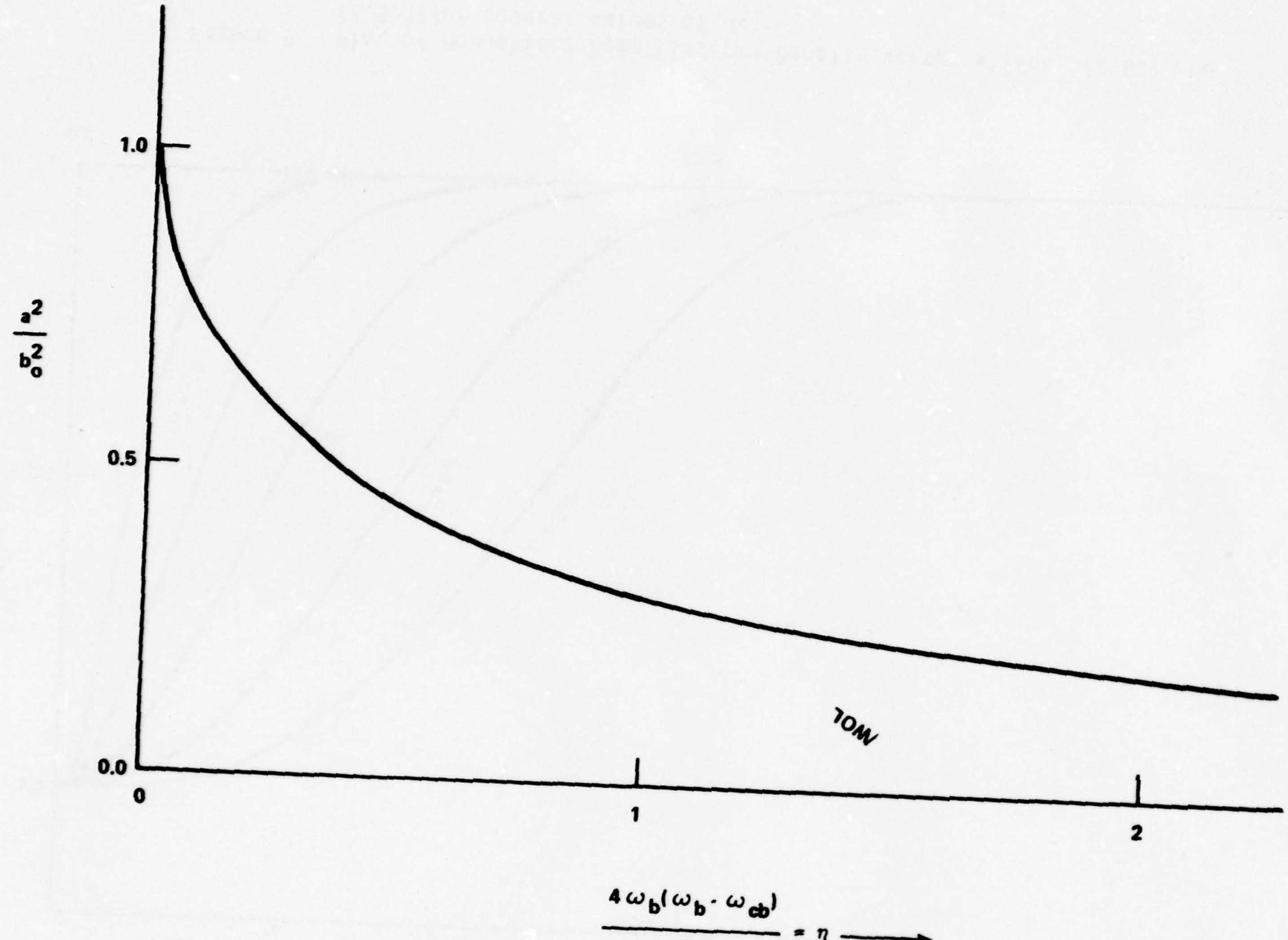

Figure 9. Plot of Normalized Effective Beam Radius-squared a^2/b_0^2 versus Parameter η for Diffused Beam Equilibrium [Eq. (2.93)]

Eq. (2.67) can be expressed in the equivalent form

$$\frac{1}{X''} \frac{\partial}{\partial X''} X'' \frac{\partial}{\partial X''} \psi(X'')=8\{\eta+\exp[-\psi(X'')]\} , \tag{2.91}$$

where

$$\eta = -\zeta = 4\omega_b(\omega_b-\omega_{cb})/K. \tag{2.92}$$

The effective beam radius is calculated numerically from

$$\frac{a^2}{b_0^2} = 2\int_0^\infty dX'' \; X''\exp[-\psi(X'')] . \tag{2.93}$$

Figure 9 shows a plot of a^2/b_0^2 versus η for $\eta \geq 0$, i.e., for radially confined equilibria with radial density profile decreasing monotonically as a function of X". Evidently, a/b_0 decreases monotonically as a function of η from the value $a/b_0=1$ when $\eta=0$ (the familiar Bennett pinch radius). Figure 10 shows a plot of $\psi(X'')$ versus $X''=r/b_0$ obtained numerically from Eq. (2.91) for various values of $\eta>0$ (radially decreasing density profile), and η in the range $0>\eta>-1$ (oscillatory density profile). The corresponding density profiles are illustrated in Figure 11. The special case where $\eta=0$ in Figure 11 corresponds to the Bennett pinch equilibrium density profile in Eq. (2.82). We note from Figure 11 that the beam density profile is an oscillatory function of $X''=r/b_0$ for η in the range $-1<\eta<0$, which corresponds to ω_b in the range $\omega_b^-<\omega_b<0$ or $\omega_{cb}<\omega_b<\omega_b^+$ [see Figure 4].

2.C Monoenergetic Beam in Beam Frame

As a third example of the uniform axial drift beam, we consider the delta-function distribution

$$f_b^0 = N\delta(H-\omega_b P_\theta-\beta_b cP_z- \frac{mc^2}{\gamma_b} -T) \tag{2.94}$$

where N is the normalization constant. Substituting Eq. (2.94) into Eq. (2.8), and making use of Eq. (2.19), we find

$$F(\psi) = (1-\psi)^{1/2} U(1-\psi) \tag{2.95}$$

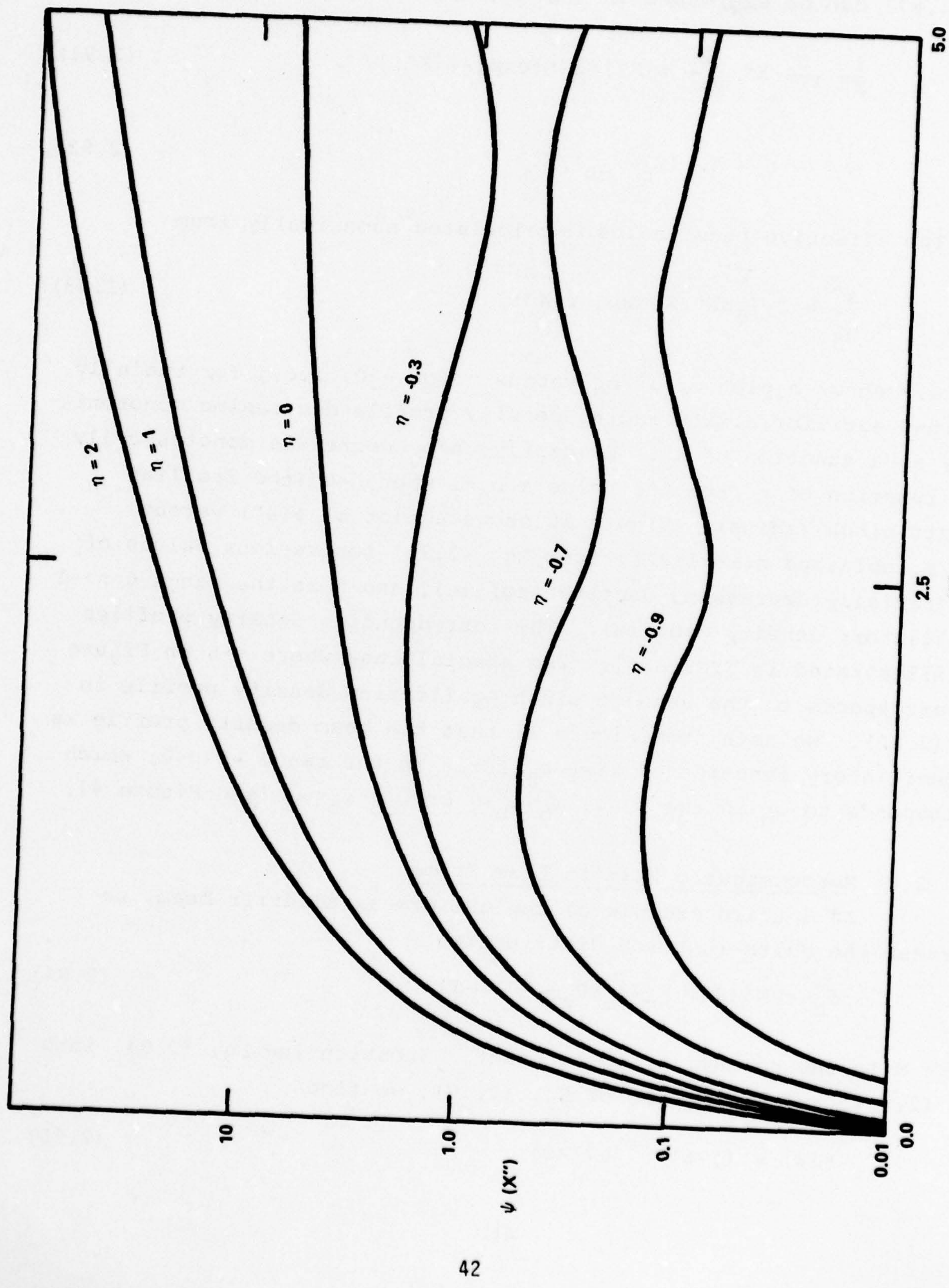

Figure 10. Plot of $\psi(x'')$ versus x'' [Eq. (2.91)] for Several Values of η.

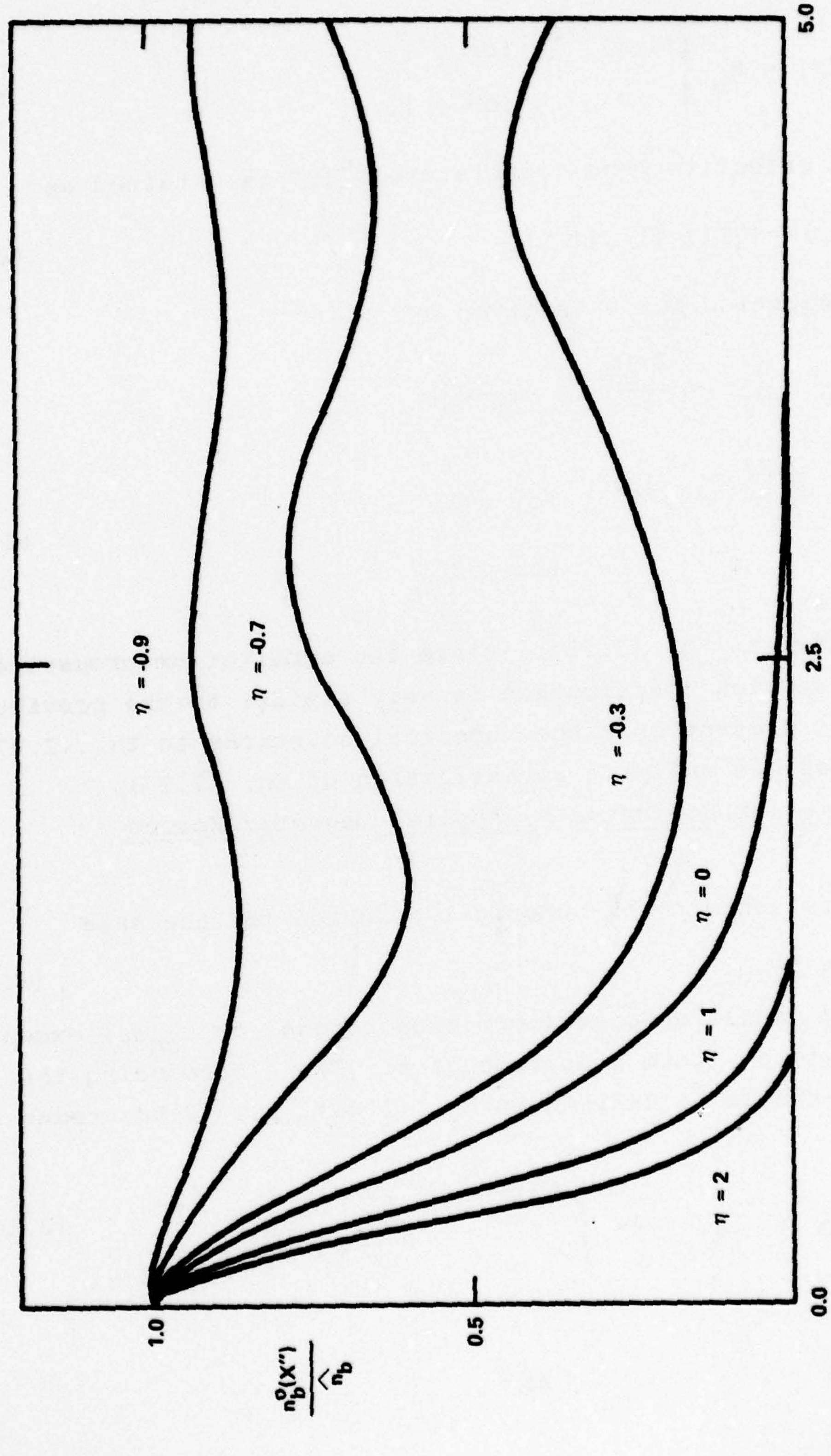

Figure 11. Plot of Normalized Beam Electron Density versus x" [Eqs. (2.66) and (2.91)] for several values of η.

where U(X) is the Heaviside step function defined in Eq. (2.34). The corresponding density profile of beam electrons is

$$n_b^0(r) = \hat{n}_b \begin{cases} (1-\psi)^{1/2}, & \text{for } \psi<1, \\ 0 & \text{, for } \psi>1. \end{cases} \tag{2.96}$$

Similarly, the effective beam temperature $T_b^0(r)$ is obtained as

$$T_b^0(r) = \frac{2}{3}T(1-\psi)\ U(1-\psi). \tag{2.97}$$

The governing equation for ψ is given by

$$\frac{1}{r}\frac{\partial}{\partial r} r \frac{\partial}{\partial r}\psi = \frac{2\gamma_b m}{T}(\omega_{cb}\omega_b-\omega_b^2)$$

$$- \begin{cases} \dfrac{\gamma_b mK}{2T}(1-\psi)^{1/2} & \text{, for } \psi<1, \\ 0 & \text{, for } \psi>1, \end{cases} \tag{2.98}$$

where K is defined in Eq. (2.23). Since the equilibrium properties for the delta-function distribution is very similar to the previous two examples, we present only the numerical solutions to Eq. (2.97), skipping the possible analytic investigation of Eq. (2.97).

(a) <u>Equilibtium Dominated by Applied Magnetic Forces $[\omega_b(\omega_{cb}-\omega_b)\geq 0]$</u>

We first obtain the numerical solution for the case

$$0 \leq \omega_b \leq \omega_{cb}, \tag{2.99}$$

when the applied magnetic force (term proportional to $\omega_{cb}\omega_b$) exceeds the centrifugal force (term proportional to ω_b^2). Introducing the dimensionless variable X' defined in Eq. (2.86), Eq. (2.98) reduces to

$$\frac{1}{X'}\frac{\partial}{\partial X'} X' \frac{\partial}{\partial X'}\psi = 4 - \begin{cases} 4\alpha(1-\psi)^{1/2}, & \psi<1, \\ 0 & ,\psi>1, \end{cases} \tag{2.100}$$

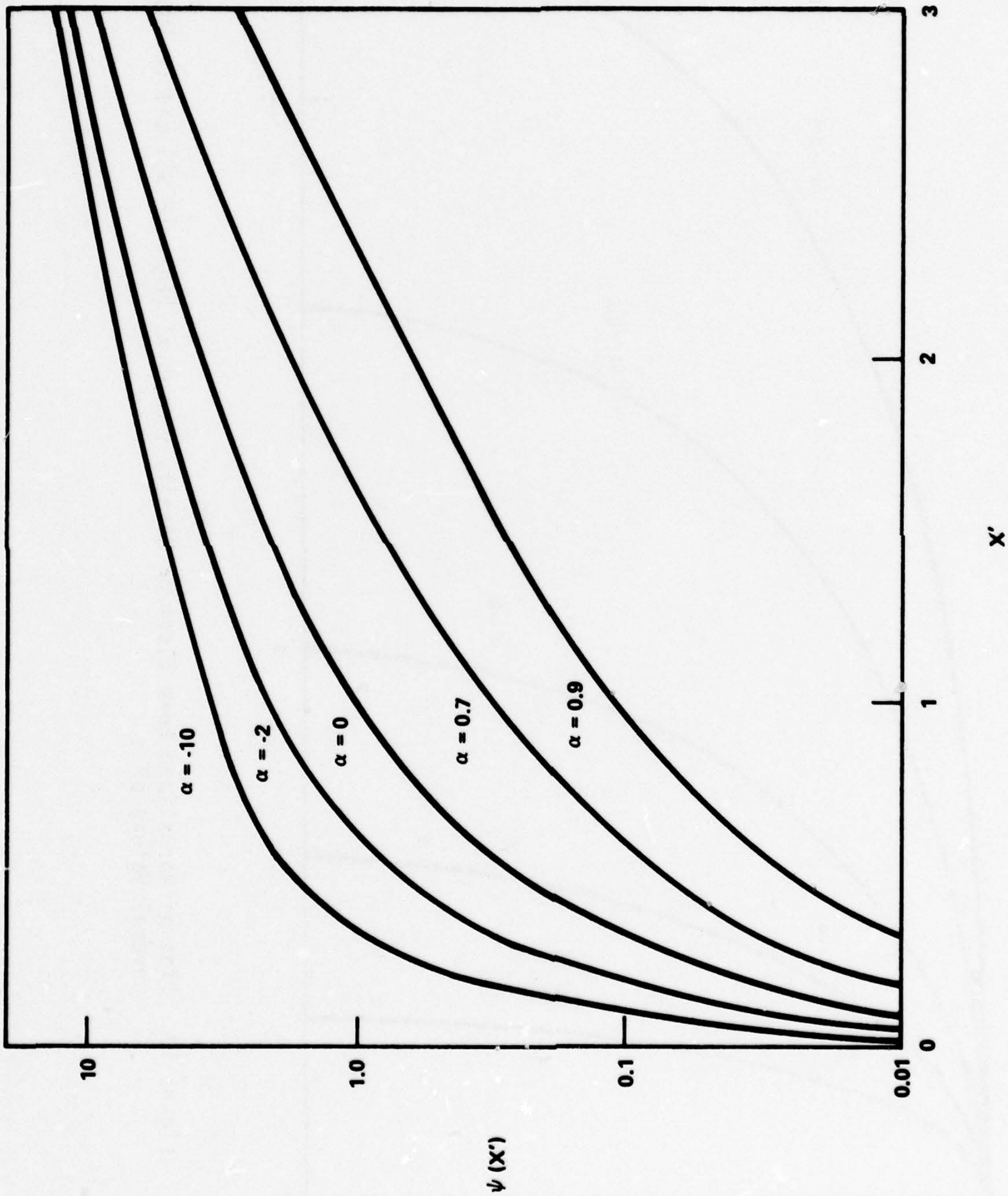

Figure 12. Plot of $\psi(x')$ versus x' [Eq. (2.100)] for Several Values of α.

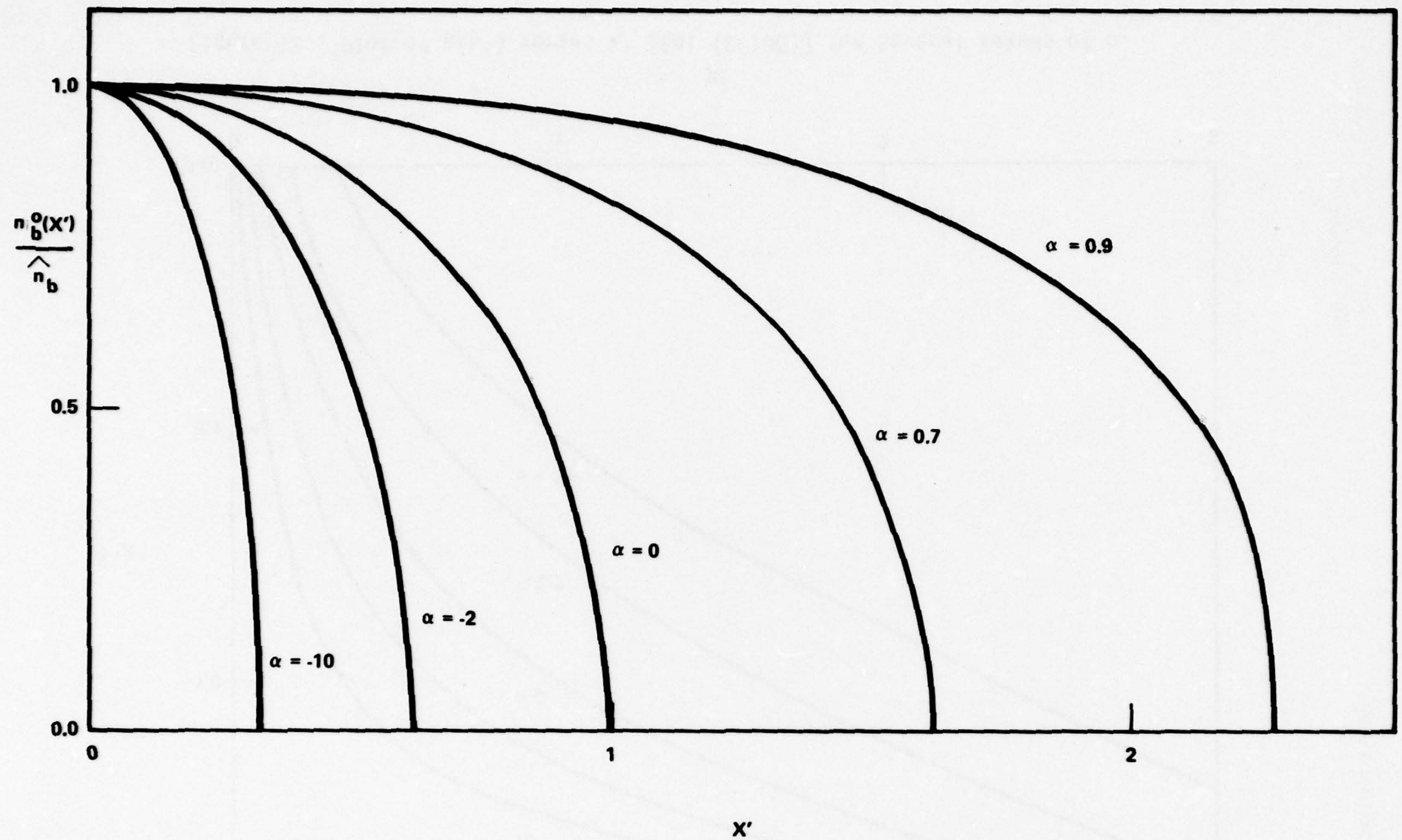

Figure 13. Plot of Normalized Beam Electron Density versus x' [Eqs. (2.96) and (2.100)] for Several Values of α.

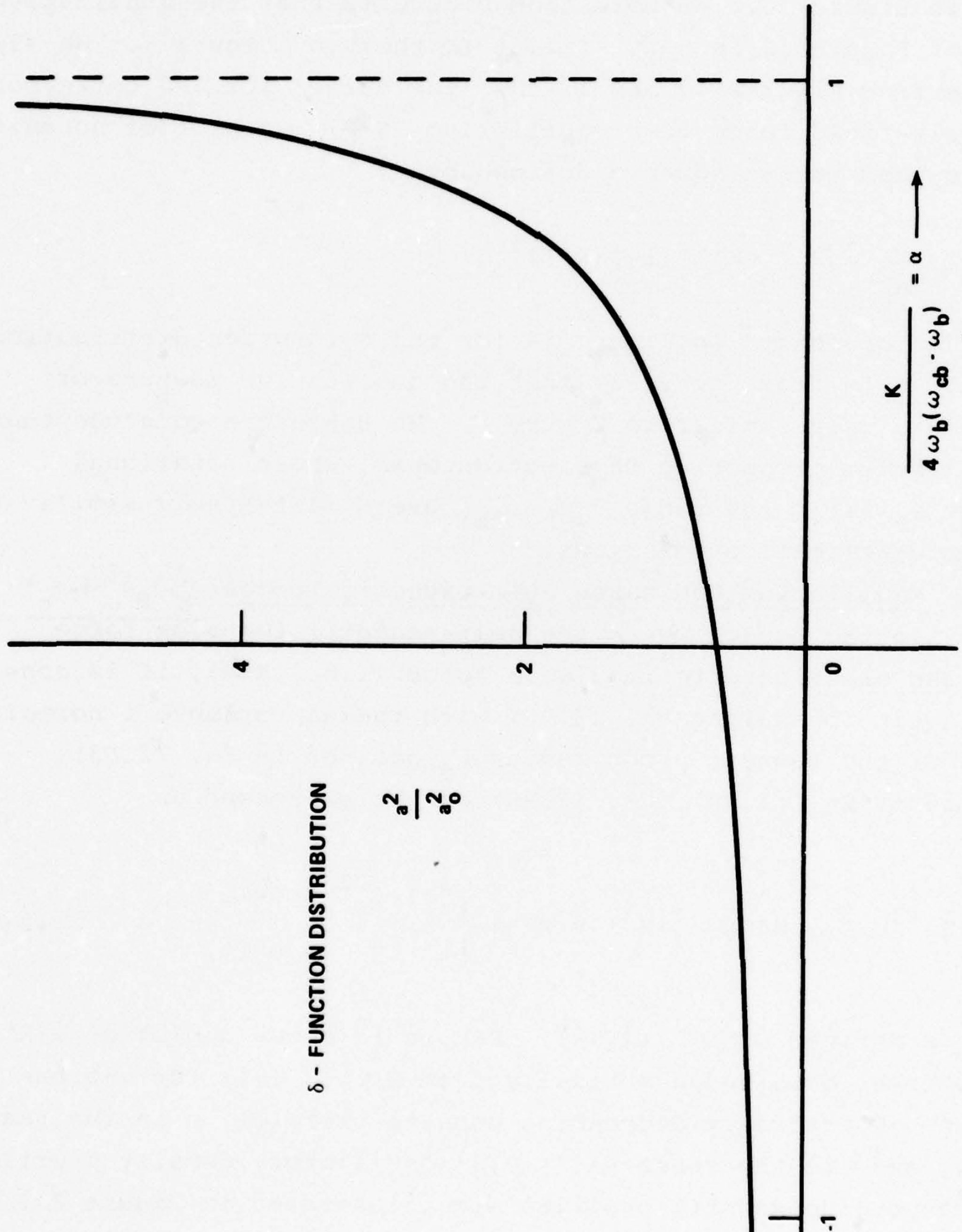

Figure 14. Plot of Normalized Effective Beam Radius-squared a^2/a_0^2 versus α for δ-Function Distribution.

where $\alpha=K/4\omega_b(\omega_{cb}-\omega_b)$ is defined in Eq. (2.88). Figure 12 is a plot of $\psi(X')$ versus $X'=r/a_0$ for several values of α. The corresponding normalized density profile $n_b^0(X')/\hat{n}_b=[1-\psi(X')]^{1/2}$ is plotted versus $X'=r/a_0$ in Figure 13. We note from Figure 12 that the qualitative feature of Figure 12 is very similar to those of Figure 7. We also emphasize from Figures 12 and 13 that the curves for $\alpha=0$ correspond to the self-field force-free equilibrium (K=0). A plot of normalized effective beam radius-squared defined by

$$\frac{a^2}{a_0^2} = 2\int_0^\infty dX'X'[1-\psi(X')]^{1/2}$$

versus α is presented in Figure 14 for the δ-function distribution function. Note from Figure 14 that the qualitative feature of Figure 14 is very similar to Figure 6. We therefore conclude that the equilibrium properties of electron beam, whose rotational frequency ω_b is in the range $0\le\omega_b\le\omega_{cb}$, are qualitatively similar for different distribution functions.

(b) <u>Equilibrium Dominated Self-Magnetic Forces</u> ($\beta_b^2-f_m\beta_b^2>1-f_e$)

In the region where the self-magnetic focusing force exceeds the electrostatic repulsive force (i.e., K<0), it is convenient again to analyze Eq. (2.98) with radial variable r normalized in units of the Bennett pinch radius b_0 defined in Eq. (2.83). Making use of Eq. (2.90), Eq. (2.98) can be expressed as

$$\frac{1}{X''}\frac{\partial}{\partial X''}X''\frac{\partial}{\partial X''}\psi(X'') = 8\eta + \begin{cases} 8(1-\psi)^{1/2}, & \psi<1, \\ 0, & \psi>1, \end{cases} \tag{2.101}$$

where η is defined in Eq. (2.92). Figure 15 shows a plot of $\psi(X'')$ versus $X''=r/b_0$ obtained numerically from Eq. (2.101) for various values of $\eta>0$ (radially decreasing density profile), η in the range $-0.5\le\eta\le0$, and η in the range $-1<\eta\le-0.5$ (oscillatory density profile). The corresponding density profiles are illustrated in Figure 16. We note from Figure 15 that the value of $\psi(X'')$ becomes exactly unity at $X''=1.4$ for $\eta=-0.5$. Therefore, we have the central and successive

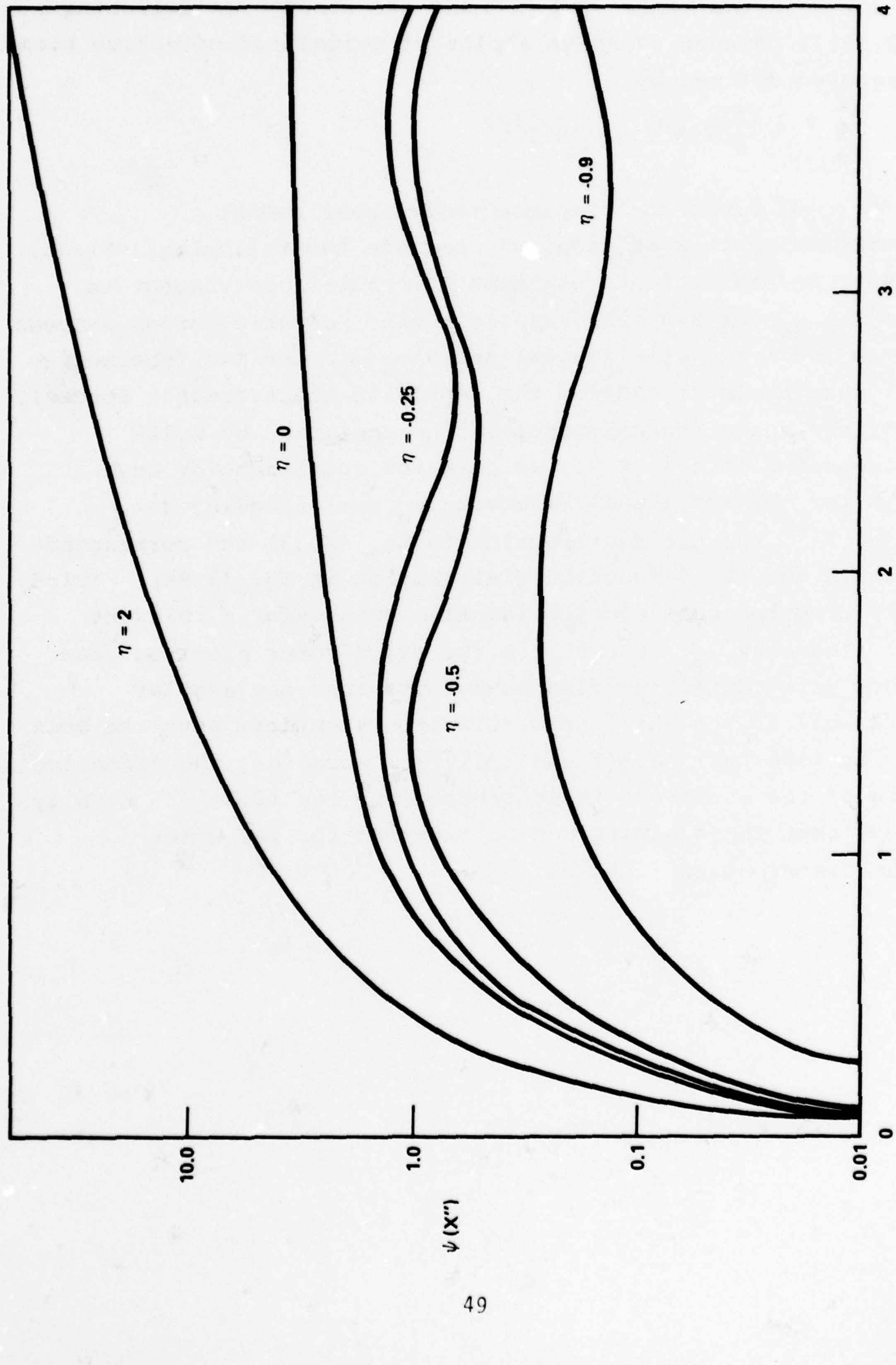

Figure 15. Plot of $\psi(x'')$ versus x'' [Eq. (2.101)] for Several Values of η.

coaxial annular beam densities for η in the range $-0.5<\eta>0$ [see Figure 16 for η in the range $-0.5<\eta<0$ and the discussion following the Eq. (2.55)]. Figure 17 shows a plot of normalized effective beam radius - squared defined by

$$\frac{a^2}{b_0^2} = 2 \int_0^\infty dX''X''[1-\psi(X'')]^{1/2}$$

versus η for $\eta>0$, i.e., for complete radial confinement.

In summerizing this section, we conclude the following. First, the necessary and sufficient condition for radial confinement is given by $\omega_b^-<\omega_b<\omega_b^+$ for $K>0$ (the repulsive electrostatic forces exceeds the focussing self-magnetic forces) and $0<\omega_b<\omega_{cb}$ for $K<0$ (the self-magnetic focussing force exceeds the repulsive electrostatic forces). Second, for the sharp boundary equilibrium dominated by self-magnetic focussing forces ($K<0$), we have the multi-annular beam equilibrium for the rotational parameter ω_b corresponding to $0<\zeta<[1-J_0(\alpha_{01})]^{-1}$ for the distribution in Eq. (2.33) and corresponding to $0<\zeta<0.5$ for the δ-function distribution in Eq. (2.94). Third, oscillatory electron beam equilibrium also exists for a relavent rotational frequency ω_b. Fourth, in the rigid-rotor electron beam with uniform axial drift, we also have found that the angular velocity as well as the axial beam velocity is uniform over the beam cross section [see Eqs. (2.11) and (2.12)]. Moreover, the effective temperature of the electrons is isotropic [see Eq. (2.14)]. Finally, we point out that the analysis can be extended for any other equilibrium distribution function.

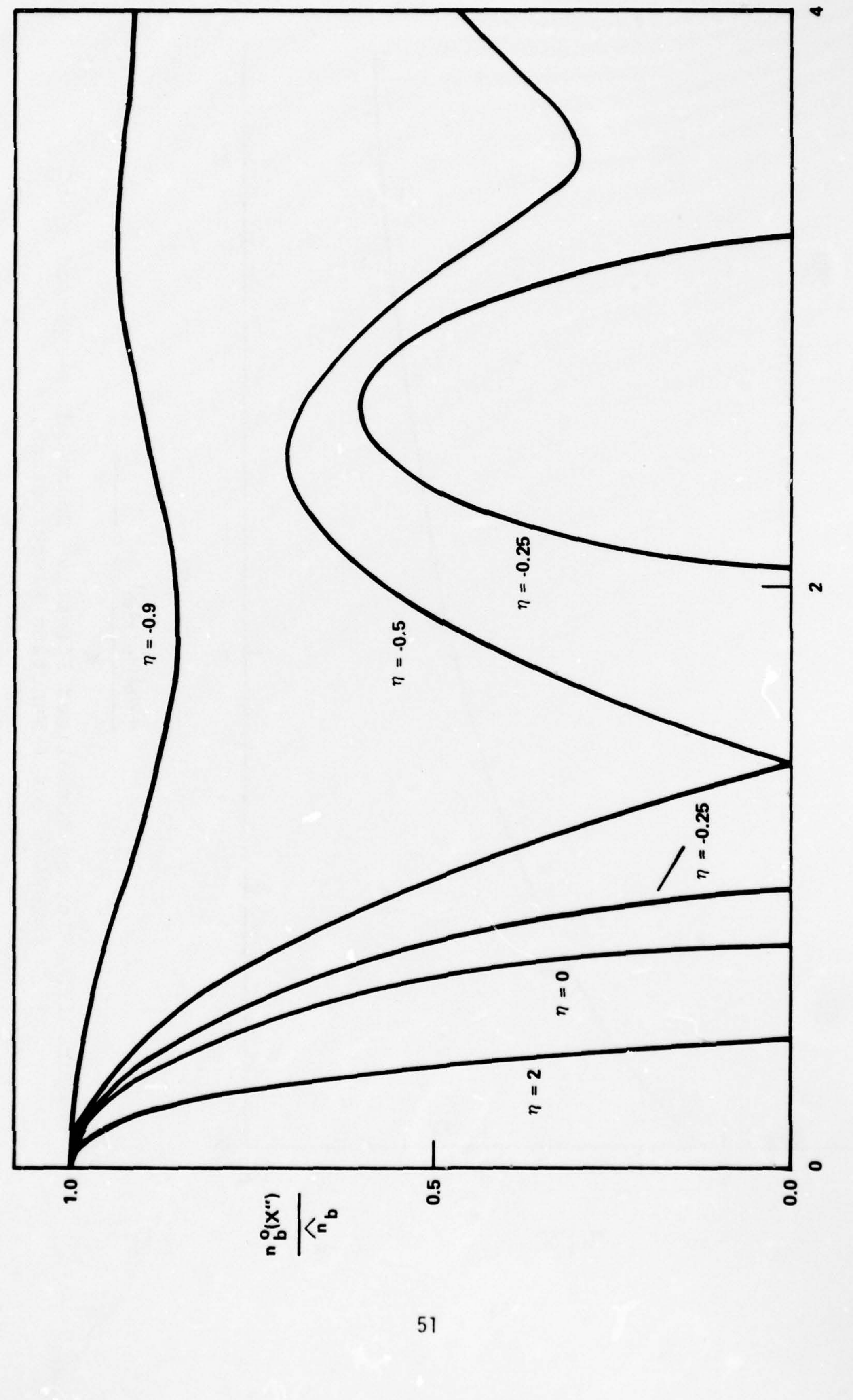

Figure 16. Plot of Normalized Beam Electron Density versus x'' [Eqs.(2.96) and (2.101)] for Several Values of η.

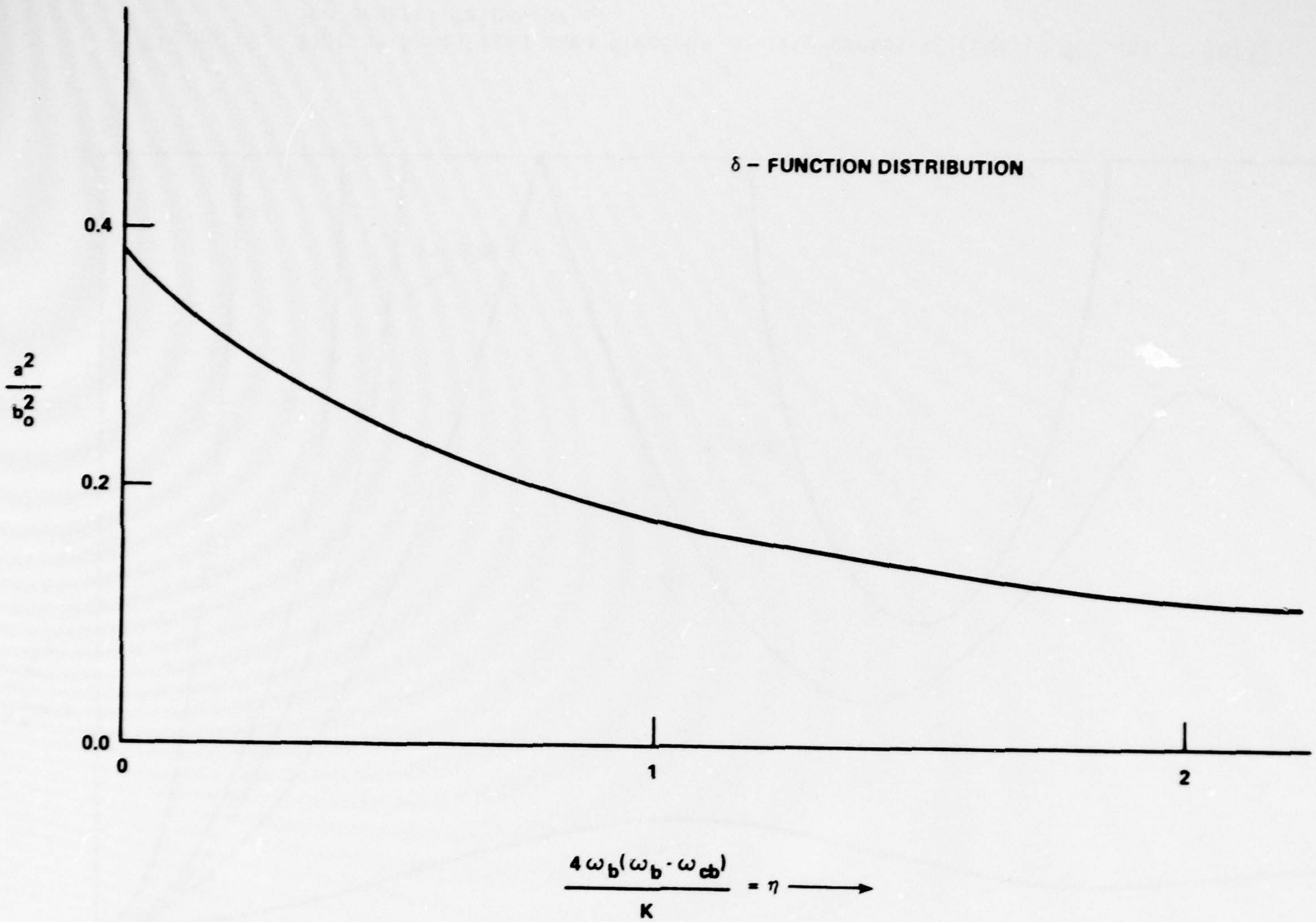

Figure 17. Plot of Normalized Effective Beam Radius-squared a^2/b_o^2 Versus η for δ-Function Distribution.

3. STIFF ELECTRON BEAM

In this section, we investigate the equilibrium properties of the stiff electron beam that is characterized by the zero axial temperature. All the electrons have the same axial canonical momentum so that the distribution function is

$$f_b^0(H-\omega_b P_\theta, P_z) = G(H-\omega_b P_\theta)\,\delta(P_z-\gamma_0 m\beta_0 c), \qquad (3.1)$$

where $\gamma_0=(1-\beta_0^2)^{-1/2}$ is a constant, and G is an arbitrary function determined by the injection condition of the electron beam. The angular velocity of beam equilibria described by Eq. (3.1) is uniform over the beam cross section. However, the axial velocity $V_{zb}^0(r)$ of the electron beam fluid element is not uniform anymore over the cross section. Making use of Eqs. (1.6) and (1.7), and the approximation $p_r^2+p_\theta^2 \ll m^2c^2$, we find

$$H - \omega_b P_\theta = \gamma_0 mc^2 + \frac{p_\perp^2}{2\gamma_z m} + \chi(r) T_\perp \qquad (3.2)$$

where the function $\chi(r)$ is defined by

$$\chi(r) = \frac{[\gamma_z(r)-\gamma_0]mc^2 - e\phi_0(r)}{T_\perp} - \frac{1}{2}m\frac{(\gamma_z\omega_b^2-\omega_b\hat{\omega}_{cb})}{T_\perp} r^2, \qquad (3.3)$$

the mass scale $\gamma_z(r)$ is defined by

$$\gamma_z(r)mc^2 = (m^2c^4+c^2p_z^2)^{\frac{1}{2}} = \{m^2c^4+c^2[\gamma_0 m\beta_0 c+\frac{e}{c}A_z^s(r)]^2\}^{\frac{1}{2}}, \qquad (3.4)$$

$p_\perp^2 = p_r^2+(p_\theta-\gamma_z m\omega_b r)^2$, $T_\perp$ = const is a measure of the transverse thermal energy spread and $\hat{\omega}_{cb}=eB_0/mc$ is the nonrelativistic electron cyclotron frequency. In obtaining Eq. (3.2), we have assumed that $A_z^s(r=0)=0=\phi_0(r=0)$ without loss of generality. Note from Eq. (3.4) that $\gamma_z(r=0)=\gamma_0$, so that $\chi(r=0)=0$ in Eq. (3.3).

Substituting Eq. (3.1) and (3.2) into Eq. (1.11) and defining

$$F(\chi)=\frac{\int_0^\infty duG[\gamma_0 mc^2+u+\chi(r)T_\perp]}{\int_0^\infty duG(\gamma_0 mc^2+u)}, \tag{3.5}$$

we find the density profile of the beam electrons to be

$$n_b^0(r) = \hat{n}_b(\gamma_z/\gamma_0)\ F[\chi(r)], \tag{3.6}$$

where $\hat{n}_b$ is the beam electron density at r=0. It is also straightforward to show from Eqs. (1.12), (3.1) and (3.2) that the axial mean momentum of a beam electron fluid element is approximated by

$$n_b^0(r)V_{zb}^0(r)=[\beta_0 c+(e/\gamma_0 mc)A_z^s(r)]\hat{n}_b F(\chi). \tag{3.7}$$

The transverse temperature of the beam electrons is defined by

$$n_b^0(r)\ \ T_\perp^0(r)=\tfrac{1}{2}\int d^3p[v_r p_r+(v_\theta-V_{\theta b}^0)(p_\theta-\langle p_\theta\rangle)]f_b^0, \tag{3.8}$$

where v_j and $\langle p_j\rangle$ are defined in Eq. (2.13). Making use of the approximation $\gamma mc^2 = (m^2c^4+c^2\underset{\sim}{p}^2)^{\frac{1}{2}} \simeq \gamma_z mc^2$, we can simplify Eq. (3.8) as

$$n_b^0(r)T_\perp^0(r) = 2\pi\gamma_z m\int_0^\infty duuG[\gamma_0 mc^2+u+\chi(r)T_\perp). \tag{3.9}$$

The axial temperature profile is obtained by substituting Eq. (3.1) into Eq. (2.15) and we find

$$T_z^0(r) = 0\,. \tag{3.10}$$

Due to the presence of the factor $\delta(p_z-\gamma_0 m\beta_0 c)$in the equilibrium distribution function, the electron motion in the axial direction is cold and the effective axial temperature is zero.

The equilibrium properties of the electron beam are determined through Eqs. (1.9), (1.10) and (3.5) - (3.7). We now analyze these equations for one specific choice of distribution fuction f_b^0, in which all electrons have the same energy in the laboratory frame. This will orient the reader and illustrate the equilibrium properties of the stiff electron beam.

As an example, we consider the delta-function distribution

$$G(H-\omega_b P_\theta) = \delta(H-\omega_b P_\theta - \gamma_0 mc^2 - T_\perp), \tag{3.11}$$

where all the beam electrons have the same energy. Substituting Eq. (3.11) into Eqs. (3.5) and (3.6), we find

$$F(\chi) = \begin{cases} 1, & \text{for } \chi \le 1, \\ 0, & \text{for } \chi > 1, \end{cases} \tag{3.12}$$

and the electron density profile

$$n_b^0(r) = \hat{n}_b \frac{\gamma_{z(r)}}{\gamma_0} \begin{cases} 1, & \text{for } \chi(r) \le 1, \\ 0, & \text{for } \chi(r) > 1. \end{cases} \tag{3.13}$$

For notational convenience in the subsequent analysis, we define the collisionless skin depth δ by

$$\delta^2 = c^2/\hat{\omega}_{pb}^2 \tag{3.14}$$

where $\hat{\omega}_{pb}^2 = 4\pi\hat{n}_b e^2/\gamma_0 m$ is the beam electron plasma frequency squared. The z-component of the vector potential $A_z^s(r)$ is determined by substituting Eqs. (3. 7) and (3.12) into Eq. (1.10). For $\chi \le 1$ we have

$$\frac{1}{r}\frac{\partial}{\partial r} r \frac{\partial}{\partial r} A_z^s(r) - \frac{1-f_m}{\delta^2} A_z^s(r) = 4\pi e n_b \beta_0 (1-f_m). \tag{3.15}$$

On the other hand, for $\chi > 1$, the vector potential $A_z^s(r)$ is determined from

$$\frac{1}{r}\frac{\partial}{\partial r} r\frac{\partial}{\partial r} A_z^s(r) = 0. \tag{3.16}$$

We assume that r_c is the beam confinement radius so that $\chi(r_c) = 1$. The solution to the Eq. (3.15) and (3.16), which is continuous at $r = r_c$, has continuous first derivative at $r = r_c$, and satisfies $A_z^s\,(r=0) = 0$, is

$$A_z^s(r) = \frac{\gamma_0 mc^2 \beta_0}{e} \begin{cases} [I_0(r\sqrt{1-f_m}/\delta)-1], & 0<r<r_c, \\ [I_0(r_c\sqrt{1-f_m}/\delta) + \frac{r_c\sqrt{1-f_m}}{\delta} I_1(r_c\sqrt{1-f_m}/\delta) \\ \quad \times \ln\frac{r}{r_c} - 1], & r>r_c, \end{cases} \tag{3.17}$$

where $I_\ell(x)$ is the modified Bessel function of the first kind of order ℓ. The corresponding self azimuthal magnetic field is given by

$$B_\theta^s(r) = -1\frac{\gamma_0 mc^2\beta_0(1-f_m)^{\frac{1}{2}}}{e\delta} \begin{cases} I_1(r\sqrt{1-f_m}/\delta), & 0>r>r_c, \\ \frac{r_c}{r} I_1(r_c\sqrt{1-f_m}/\delta), & r>r_c. \end{cases} \tag{3.18}$$

Substituting Eq. (3.17) into Eq. (3.7) gives the mean axial velocity profile

$$V_{zb}^0(r) = \frac{\gamma_z(r)}{\gamma_0}\beta_0 c\, I_0(r\sqrt{1-f_m}/\delta), \tag{3.19}$$

where $\gamma_z(r)$ is given by

$$\gamma_z(r) = [1+\gamma_0^2\beta_0^2\, I_0\,(r\sqrt{1-f_m}/\delta)^2]^{\frac{1}{2}} \tag{3.20}$$

The electrostatic potential $\phi_0(r)$ is determined from

$$\frac{1}{r}\, r\frac{\partial}{\partial r} r\frac{\partial}{\partial r}\phi_0(r) = 4\pi e(1-f_e)\,\hat{n}_b(\gamma_z/\gamma_0)\begin{cases}1, & \chi(r)\le 1,\\ 0, & \chi(r)>1.\end{cases} \tag{3.21}$$

The exact solution to Eq. (3.21) is not tractable analytically; however, the asymptotic solution to Eq. (3.21) can be obtained in various limits of practical interest, depending on the size of the self-field influence.

3 Tenuous Beam

In circumstances where the beam density is so low that

$$\frac{\nu}{\gamma_0} = \frac{N_b e^2}{\gamma_0 mc^2} \simeq \frac{1}{4}\left(\frac{r_c}{\delta}\right)^2 \ll 1, \tag{3.22}$$

the modified Bessel function $I_0(x)$ can be expanded according to $I_0(x) = 1+x^2/4$, giving

$$(\gamma_z(r)/\gamma_0) = 1+r^2\beta_0^2(1-f_m)/4\delta^2 \tag{3.23}$$

The electrostatic potential in Eq. (3.21) can also be approximated by

$$\phi_0(r) = \pi e(1-f_e)\hat{n}_b r^2. \tag{3.24}$$

Substituting Eqs. (3.23) and (3.24) into Eq. (3.3), the dimensionless function $\chi(r)$ is given by

$$\chi(r) = \frac{\gamma_0 m}{2T_\perp}(\omega_b^+-\omega_b)(\omega_b-\omega_b^-)r^2 \tag{3.25}$$

where the laminar cold-fluid rotation frequencies $\omega_b^\pm$ are defined by

$$\omega_b^\pm = \frac{1}{2}\left\{(\hat{\omega}_{cb}/\gamma_0) \pm[(\hat{\omega}_{cb}/\gamma_0)^2-K]^{1/2}\right\}, \tag{3.26}$$

in which

$$K = 4\omega_b^+\omega_b^- = 2\hat{\omega}_{pb}^2[1-f_e-\beta_0^2+f_m\beta_0^2] \tag{3.27}$$

The necessary and sufficient condition for a radially confined equilibrium is given by

$$\omega_b^- < \omega_b < \omega_b^+ \tag{3.28}$$

from Eq. (3.25). The radial confinement radius r_c is derived from $\chi(r_c)=1$ and given by

$$r_c = \left[\frac{2T_\perp}{\gamma_0 m(\omega_b^+-\omega_b)(\omega_b-\omega_b^-)}\right]^{1/2} \tag{3.29}$$

Equation (3.29) indicates that the beam radius r_c increases when the beam temperature $T_\perp$ increases. Moreover, in the event that ω_b is closely tuned to either ω_b^+ or ω_b^-, the two laminar cold-fluid rotation frequencies, the beam radius r_c becomes very large. It is worthwhile to note the difference between the radial confinement condition in the previous section and that in this section. For the electron beam with uniform axial drift described in Section 2, the necessary and sufficient condition for a radially confined equilibrium dominated by the self-magnetic force ($K<0$) is given by $0<\omega_b<\omega_{cb}$ and we have oscillatory equilibria for $K<0$ and rotational frequency ω_b in the range $\omega_{cb}<\omega_b<\omega_b^+$ or $\omega_b^-<\omega_b<0$. However, the stiff monoenergetic electron beam is radially confined even if $K<0$ and the rotational frequency ω_b is in the range $\omega_{cb}<\omega_b<\omega_b^+$ or $\omega_b^-<\omega_b<0$. The reason for this difference is simply that the current source $n_b^0(r)V_{zb}^0(r)$ in Eq. (3.7) for the vector potential $A_z^s(r)$ has one more additional term, which is proportional to $A_z^s(r)$ in the right-hand side of Eq. (3.7). This term ensures that the vector potential $A_z^s(r)$ in Eq. (3.15) increases monotonically by increasing r. On the other hand, in the electron beam with uniform axial drift, the current source $n_b^0(r)V_{zb}^0$ in Eq. (2.10) doesn't include the term proportional to $A_z^s(r)$, and thereby leads to an oscillatory equilibrium for K<0 and for $\omega_{cb}<\omega_b<\omega_b^+$ or $\omega_b^-<\omega_b<0$.

3.B <u>Space-Charge Neutralized Beam</u>

As a second example of finding an analytic expression of the dimensionless function $X(r)$ in Eq. (3.3) for a monoenergetic beam, we consider the space-charge neutralized beam, i.e.,

$$f_e = 1, \tag{3.30}$$

which ensures the elimination of the electrostatic potential in Eq. (3.3). Therefore, in order to have a radially confined equilibrium, it is required that

$$\frac{\gamma_z(r)}{\gamma_0} \geq g(r^2) = 1 + \frac{\dfrac{T_\perp}{\gamma_0 mc^2} - \dfrac{1}{2}\dfrac{\omega_b(\omega_{cb}-\omega_b)r^2}{c^2}}{1 - \dfrac{1}{2}\dfrac{\omega_b^2}{c^2}r^2} \tag{3.31}$$

for $r>r_c$, where r_c is the radial confinement radius satisfying $\gamma_z(\gamma_c)/\gamma_0 = g(r_c^2)$. Here $\gamma_z(r)$ is defined in Eq. (3.4). We can find from Eq. (3.31) that the function $g(r^2)$ is a monotonically increasing or decreasing function of r^2 accordingly as

$$T_\perp \omega_b^2/\gamma_0 mc^2 \gtrless \omega_b(\omega_{cb}-\omega_b).$$

Since the whole analysis in this paper is valid only when $(\omega_b r/c)^2 \ll 1$ [see Eq. (1.3)], Eq. (3.31) is also valid only when $(\omega_b r/c)^2 \ll 1$. Note from Eq. (3.31) that in case $\omega_b(\omega_{cb}-\omega_b) > T_\perp\omega_b^2/\gamma_0 mc^2$, we always have a radially confined equilibrium even without the self-pinching forces (i.e.,

$\gamma_z(r)\simeq\gamma_0$). Even for the case $T_\perp\omega_b^2/\gamma_0 mc^2>\omega_b(\omega_{cb}-\omega_b)$, a radially confined equilibrium can exist, provided there is a reasonable self-magnetic pinching force. However, finding the exact r_c requires the numerical analysis of Eq. (3.31).

3.C Equilibrium with $\omega_b = 0$.

The equilibrium properties of electron beams with $\omega_b=0$ and described by Eq. (3.11) have been investigated in the previous literature.[3] Thus, we repeat here some of the arguments made in previous studies.[3] In the case of $\omega_b=0$, the dimensionless function on $\chi(r)$ can be simplified to

$$\chi(r) = \frac{[\gamma_z(r)-\gamma_0]mc^2-e\phi_0(r)}{T_\perp} \tag{3.32}$$

The density profile is given by

$$\begin{aligned} n_b^0(r) &= [1 + \frac{e\phi_0}{\gamma_0 mc^2+T_\perp}]\hat{n}_b, \quad r<r_c, \\ &\simeq (1 + \frac{e\phi_0}{\gamma_0 mc^2})\hat{n}_b, \quad r<r_c \end{aligned} \tag{3.33}$$

Substituting Eq. (3.33) into Eq. (1.9) gives

$$\frac{1}{r}\frac{\partial}{\partial r} r\frac{\partial}{\partial r}\phi_0(r) = \begin{cases} 4\pi(1-f_e)\hat{n}_b[1+\frac{e\phi_0(r)}{\gamma_0 mc^2}], & 0<r<r_c, \\ 0 & , r>r_c. \end{cases} \tag{3.34}$$

The solution to Eq. (3.34) is

$$\phi_0(r)=\frac{\gamma_0 mc^2}{e}\begin{cases} [I_0(r\sqrt{1-f_e}/\delta)-1], & 0<r<r_c, \\ [I_0(r_c\sqrt{1-f_e}/\delta)+\frac{r_c\sqrt{1-f_e}}{\delta} I_1(r_c\sqrt{1-f_e}/\delta)\ln\frac{r}{r_c}-1], & r>r_c \end{cases} \tag{3.35}$$

From Eq. (3.35), the radial electric field $E_r^0(r)=-\partial\phi_0/\partial r$ can be expressed as

$$E_r^0(r) = -\frac{\gamma_0 mc^2 (1-f_e)^{\frac{1}{2}}}{e\delta} \begin{cases} I_1(r\sqrt{1-f_e}/\delta), & 0<r<r_c, \\ \frac{r_c}{r} I_1(r_c\sqrt{1-f_e}/\delta), & r>r_c. \end{cases} \tag{3.36}$$

The additional equilibrium properties are obtained from Eq. (3.32) by substituting Eqs. (3.4), (3.17) and (3.35) into Eq. (3.32). However, this is not straightforward and requires some numerical calculation.

We conclude this section by deriving some general properties. First the perpendicular temperature of beam electrons defined in Eq. (3.9) can be expressed as

$$T_\perp^0(r) = T_\perp[1 - \lambda(r)] \tag{3.37}$$

It is also straightforward to calculate the total current carried by the electron beam for the equilibrium distribution function defined in Eq. (3.11). Making use of Eqs. (3.13) and (3.19), we can express the <u>magnitude</u> of the total beam current as

$$I = 2\pi e \int_0^{r_c} dr r n_b^0(r) V_{zb}^0(r) = (mc^3/e) \frac{r_c\sqrt{1-f_m}}{2\delta} \beta_0 \gamma_0 I_1\left(\frac{r_c\sqrt{1-f_m}}{\delta}\right)$$

$$\simeq 17000 \beta_0 \gamma_0 \frac{r_c\sqrt{1-f_m}}{2\delta} I_1\left[\frac{r_c\sqrt{1-f_m}}{\delta}\right] \text{ amperes} \tag{3.38}$$

when use has been made of $mc^3/e = 17000$ in units of amperes. Evidently, I in Eq. (3.38) is sensitive to the value of r_c/δ. The analysis in this section can also be extended to a diffuse electron beam equilibrium described by the equilibrium distribution function

$$G(H-\omega_b P_\theta) = \exp\{-(H-\omega_b P_\theta - \gamma_0 mc^2)/T_\perp\} \quad . \tag{3.39}$$

The resulting equations are again two coupled second order differential equations. However, an analysis of these equations can also be carried out in a relatively straightforward manner.

4. CONCLUSIONS

In this paper, we have investigated the equilibrium properties of a rigid-rotor relativistic intense electron beam described by the equilibrium distribution function of the form $f_b^0(H,P_\theta,P_z) = f_b^0(H-\omega_b P_\theta,P_z)$ which ensures a rigid-rotor equilibrium with the angular frequency ω_b. The theoretical analysis of relativistic electron beams has been carried out, neglecting the atomic process and discrete particle interactions (i.e., binary collisions), because the collective processes are assumed to dominate on the time and length scale of interest. The positive ions have been assumed to be immobile, providing partial space-charge neutralization.

Various equilibirum properties were calculated in Section 2, for a relativistic electron beam with uniform axial drift velocity. A second order differential equation (2.20) has been obtained for the dimensionless function $\psi(r)$ which governs the equilibrium properties of the electron beam. We have investigated this differential equation analytically and numerically for several specific examples of the electron distribution function, thereby finding the necessary and sufficient condition for a radially confined equilibrium. One of the important features for rigid-rotor electron beam with uniform axial drift is that an oscillatory equilibrium exists for the rotational frequency in the range $\omega_{cb}<\omega_b<\omega_b^+$ or $\omega_b^-<\omega_b<0$. Moreover, the effective temperature profile is isotropic for this distribution function.

In Section 3, the equilibrium properties were calculated for a stiff electron beam, in which all the beam electrons have the same axial canonical momentum, thereby leading to a zero axial temperature. Particularly, the monoenergetic electron beam properties have been analytically investigated in detail. The expression for total current carried by the monoenergetic electron beam was derived in terms of the beam intensity. However, the governing equations for a stiff electron beam are two coupled second order differential equations, and the analysis of these equations is considerably more complicated than that of an electron beam with uniform axial drift.

ACKNOWLEDGEMENTS

It is a pleasure to acknowledge the benefit of useful discussions with Drs. Ronald C. Davidson and Georege E. Hudson. This research was supported by Independent Research (I.R.).

REFERENCES

1. Davidson, R. C., Theory of Nonneutral Plasma (Benjamin, Reading, MA., 1974).

2. Bennett, W. H., "Magnetically Self-Focussing Streams," Phys. Rev. 45, 1934, p. 890.

3. Hammer, D. A., and Rostoker, N., "Propagation of High Current Relativistic Electron Beams," Phys. Fluids 13, 1970, p. 1831.

4. Gratreau, P., "Generalized Bennett Equilibria and Particle Orbit Analysis of Plasma Columns Carrying Ultra-High Currents," Phys. Fluids 21, 1978, p. 1302.

5. Davidson, R. C., and Uhm, H. S., "Thermal Equilibrium Properties of an Intense Relativistic Electron Beam," Phys. Fluids, in press 1979.

6. Armstrong, C. M., Hammer, D. A., and Trivelpiece, A. W., "Nonneutral Electron Plasma With a 2.5 MeV Mean Energy," Phys. Lett. A55, 1976, p. 413.

7. Davidson, R. C., and Uhm, H. S., "Influence of Strong Self-Electric Fields on Ion Resonance Instability in a Nonneutral Plasma Column," Phys. Fluids, 20. 1977, p. 1938.

8. Davidson, R. C., and Uhm, H. S., "Influence of Finite Ion Lamor Radius Effects on the Ion Resonance Instability in a Nonneutral Plasma Column," Phys. Fluids, 21, 1978, p. 60.

9. Striffler, C. D., Papetnnakos, C. A., and Davidson, R. C., "Equilibrium Properties of a Rotating Nonneutral E Layer in a Cusped Magnetic Field," Phys. Fluids, 18, 1975, p. 1374.

10. Destler, W. W., Uhm, H. S., Kim, H., and Reiser, M. P., "Study of Collective Ion Acceleration in Vacuum" J. Appl. Phys., in press (1979).

11. Sloan, M. W., and Drummond, W. E., "Autoresonant Accelerator Concept," Phys. Rev. Lett. 31, 1973, p. 1234.

12. Sprangle, P., Drobot, A., and Manheimer, W., "Collective Ion Acceleration in a Converging Wave Guide," Phys. Rev. Lett. 36, 1976, p. 1180.

13. Granatstein, V. L., Sprangle, P., Parker, R. K., Pasour, J., Herndon, M., Schlesinger, S. P., and Sefter, J. L., "Realization of Relativistic Mirror; Electromagnetic Backscattering from the Front of a Magnetized Relativistic Electron Beam," Phys. Rev. A14, 1976, p. 1194.

14. Flyagin, V. A., Gaponov, A. V., Petelin, M. I., and Yulpatov, V. K., "The Gyroton," IEEE Trans. Microwave Theory and Techniques, MTT-25, 1977, p. 514.

15. Uhm, H. S., and Davidson, R. C., "Quasi-Linear Theory of Cyclotron Maser Instability," Phys. Fluids 22, in press (1979) and references therein.

16. Reiser, M. "Laminar-Flow Equilibria and Limiting Currents in Magnetically Focused Relativistic Beams", Phys. Fluids 20, 477 (1977).

17. Kligman, R. L., "Electric Conductivity in a Beam, Plasma System," NSWC/WOL TR 77-146, 15 Sep 1977.

18. Briggs, R. J., Hester, R. E., Lauer, E. J., Lee, E. P., and Spoerlein, R. L., "Radial Expansion of Self-Focused, Relativistic Electron Beams," Phys. Fluids, 19, 1976, p. 1007.

19. Lee, E. P., "Kinetic Theory of a Relativistic Beam," Phys. Fluids, 19, 1976, p. 60.

20. Lampe, M., "Energy Moment Method for Straggling of an Ultra-Relativistic Electron Beam," NRL Memorandum Report 3221, Feb. 1976.

DISTRIBUTION

Copies

Director
Defense Advanced Research Projects Agency
Attn: Dr. J. Mangano
1400 Wilson Boulevard
Arlington, Virginia 22209

Naval Research Laboratory
Attn: Dr. M. Lampe
Dr. J. Siambis
Washington, D. C. 20365

Air Force Weapons Laboratory
Kirtland Air Force Base
Attn: MAJ H. Dogliani
Albuquerque, New Mexico 87117

U. S. Army Ballistic Research Laboratory
Aberdeen Proving Ground
Attn: Dr. D. Eccleshall (DRDAR-BLB)
Aberdeen, Maryland 21005

Ballistic Missile Defense Advanced Technology Center
Attn: Dr. L. J. Havard (BMDSATC-1)
P. O. Box 1500
Huntsville, Alabama 35807

Department of Energy
Attn: Dr. T. Godlove (C-404)
Washington, D. C. 20545

National Bureau of Standards
Attn: Dr. Mark Wilson
Gaithersburg, Maryland 20760

Austin Research Associates, Inc.
Attn: Dr. W. E. Drummond
1901 Rutland Drive
Austin, Texas 78758

B-K Dynamics, Inc.
Attn: Dr. R. Linz
15825 Shady Grove Road
Rockville, Maryland 20850

The Charles Stark Draper Laboratory, Inc.
Attn: Dr. E. Olsson
555 Technology Square
Cambridge, Massachusetts 02139

IRT Corporation
Attn: Mr. W. Selph
P. O. Box 81087
San Diego, California 92138

University of California
Lawrence Livermore Laboratory
Attn: Dr. R. J. Briggs
Dr. E. Lee
P. O. Box 808
Livermore, California 94550

Los Alamos Scientific Laboratory
Attn: Dr. G. Best
P. O. Box 1663
Los Alamos, New Mexico 87545

Mission Research Corporation
Attn: Dr. C. Longmire
735 State Street
Santa Barbara, California 93102

Physical Dynamics, Inc.
Attn: Dr. K. Brueckner
P. O. Box 977
La Jolla, California 92037

Science Applications, Inc.
Attn: Dr. M. P. Fricke
1200 Prospect Street
La Jolla, California 92037

Science Applications, Inc.
Attn: Dr. R. Johnston
2680 Hanover Street
Palo Alto, California 94304

Sandia Laboratories
Attn: Mail Services Section for:
Dr. R. B. Miller
Albuquerque, New Mexico 87115

Defense Documentation Center
Cameron Station
Alexandria, Virginia 22314 12

NDW-NSWC(W)-5605/1 (Rev. 5-78)

TO AID IN UPDATING THE DISTRIBUTION LIST FOR NAVAL SURFACE WEAPONS CENTER, WHITE OAK TECHNICAL REPORTS PLEASE COMPLETE THE FORM BELOW:

TO ALL HOLDERS OF NSWC/WOL TR 78-182
by Han S. Uhm, Code R-41

DO NOT RETURN THIS FORM IF ALL INFORMATION IS CURRENT

A. FACILITY NAME AND ADDRESS *(OLD) (Show Zip Code)*

NEW ADDRESS *(Show Zip Code)*

B. ATTENTION LINE ADDRESSES:

C.

☐ REMOVE THIS FACILITY FROM THE DISTRIBUTION LIST FOR TECHNICAL REPORTS ON THIS SUBJECT.

D.

NUMBER OF COPIES DESIRED ______________________

GPO 930-784

DEPARTMENT OF THE NAVY
NAVAL SURFACE WEAPONS CENTER
WHITE OAK, SILVER SPRING, MD. 20910

OFFICIAL BUSINESS
PENALTY FOR PRIVATE USE, $300

POSTAGE AND FEES PAID
DEPARTMENT OF THE NAVY
DOD 316

COMMANDER
NAVAL SURFACE WEAPONS CENTER
WHITE OAK, SILVER SPRING, MARYLAND 20910

ATTENTION: CODE R-41